JOURNAL OF GEOPHYSICAL RESEARCH, VOL. 111, A09104, doi:10.1029/2005JA011449, 2006

Click Here for Full Article

A new shock fitting procedure for the MHD Rankine-Hugoniot relations for the case of small He^{2+} slippage

C. C. Lin,[1] J. K. Chao,[1] L. C. Lee,[1] L. H. Lyu,[1] and D. J. Wu[2]

Received 29 September 2005; revised 2 June 2006; accepted 8 June 2006; published 16 September 2006.

[1] To study MHD shocks in space, it is important to find the shock frame of reference from the observed plasma and magnetic field parameters. These shock parameters have to satisfy the Rankine-Hugoniot relations. In this study we present a novel procedure for shock fitting of the one-fluid anisotropic Rankine-Hugoniot relations and of the time difference between two spacecraft observations in the case of small He^{2+} slippage. Here, a Monte-Carlo calculation and a minimization technique are used. The observed variables including the upstream and downstream magnetic fields, plasma densities, plasma betas, plasma anisotropies, **W** (the difference between the downstream and upstream velocities, $\mathbf{W} \equiv \mathbf{V}_2 - \mathbf{V}_1$), and Δt (the time difference between two spacecraft observations) are used in our procedure where **V** is defined as the center of mass velocity of plasmas. A loss function based on a difference between the calculated and the observed values is defined, and the best fit solution is found by searching for the minimum loss function value. For shocks that cannot be fitted well, we introduce two new parameters in the modified RH relations, one in the normal momentum flux and the other in the energy flux equations. These two parameters are interpreted as the equivalent ''normal momentum'' and ''heat'' fluxes needed in the RH relations. They provide two degrees of freedom in the system, and their amounts can be estimated from our procedure. Several synthetic shocks are given to verify our procedure. We also apply this procedure to two interplanetary shocks observed by both the WIND and Geotail spacecraft. The results demonstrate that our method works for both the synthetic and the real shocks. We have shown that our method can provide accurate shock normal estimations for perpendicular and parallel shocks as well. Given that our model is based on the RH relations that do not include the effect of alpha particle (He^{2+}) slippage, it can only be applied to the cases with an ignorable slippage pressure tensor. We have investigated the pressure tensor due to alpha particle slippage using the WIND spacecraft data. It is found that in general the slippage pressure is small in comparison with the thermal pressure of the system and can be ignored. Thus our model can be applied to most interplanetary shocks observed near the ecliptic plane. However, when the slippage pressure is large, the magnetic coplanarity theorem is not valid any more. A more general model that involves slippage pressure tensor is a major and important development that is beyond the scope of the present study.

Citation: Lin, C. C., J. K. Chao, L. C. Lee, L. H. Lyu, and D. J. Wu (2006), A new shock fitting procedure for the MHD Rankine-Hugoniot relations for the case of small He^{2+} slippage, *J. Geophys. Res.*, *111*, A09104, doi:10.1029/2005JA011449.

1. Introduction

[2] Shock fitting problems have been studied for more than 3 decades. One main problem related to shock fitting is to search for an accurate shock frame of reference. This is particularly important for interplanetary (IP) shocks. The prediction of the arrival of a shock is helpful in particular for predicting the arrival of the associated magnetic cloud from the Sun. On the other hand, an accurate shock frame of reference can give accurate shock parameters (e.g., Mach number, ratio of compressions, etc.), which allows us to find the essential physics associated with the IP shock-magnetosphere interaction.

[3] In searching for an accurate shock frame of reference, determining the shock normal (direction of the shock frame) is the most important task. Many authors have worked on the shock fittings necessary to find an accurate shock normal vector using single spacecraft data. The method first proposed was the magnetic coplanarity theorem in isotropic plasmas [*Colburn and Sonett*, 1966]. This theorem demonstrates that the magnetic fields on both sides of a shock and the shock normal vector lie on the same plane. The magnetic coplanarity theorem has also been generalized for anisotropic plasmas [*Chao*, 1970]. This coplanarity theorem is frequently used to find the shock normal vector

[1]Institute of Space Science, National Central University, Taiwan.
[2]Purple Mountain Observatory, Academic Sinica, Nanjing, China.

Copyright 2006 by the American Geophysical Union.
0148-0227/06/2005JA011449$09.00

from the observed magnetic fields [e.g., *Chao and Goldstein*, 1972; *Chao and Hsieh*, 1984; *Winterhalter et al.*, 1985; *Wu et al.*, 2000].

[4] The shock normal vector can also be determined by the minimum variance method (MVA), which is based on the conservation of the normal component of the magnetic field across the shock layer [*Sonnerup and Cahill*, 1967]. This method, however, has been applied mainly to tangential and rotational discontinuities [e.g., *Lepping and Behannon*, 1980; *Sonnerup et al.*, 2004]. Recently, *Knetter et al.* [2003, 2004] suggested that the MVA is much less reliable than has been previously assumed. When applied to shock waves, it is well-known that the eigenvector degeneracy of the MVA causes that the method is not useful for finding the normal of the shock. In order to remedy this difficulty, *Scudder* [2005] proposed a novel scheme called CVA (coplanarity variance analysis), which in the search for an accurate geometry exploits the eigenvalue degeneracy in MVA, at planar structures, to enforce coplanarity. It is found that CVA is much better than MVA at finding the shock normal.

[5] *Abraham-Shrauner* [1972] proposed a mixed data method, called velocity-magnetic field coplanarity. It requires the velocity difference to lie on the same plane constructed by the magnetic fields and the shock normal vector. The expression is written as

$$\hat{n} = \pm \frac{\mathbf{B}_1 \times (\mathbf{V}_2 - \mathbf{V}_1) \times (\mathbf{B}_2 - \mathbf{B}_1)}{|\mathbf{B}_1 \times (\mathbf{V}_2 - \mathbf{V}_1) \times (\mathbf{B}_2 - \mathbf{B}_1)|}. \quad (1)$$

The velocity and magnetic field data on both sides of the shock are employed to obtain the shock normal vector. This property is consistent with the property derived by *Chao* [1970] [see *Chao*, 1970, equation (4.5)]. An approximation of the equation (1) has been derived by *Abraham-Shrauner* [1972] as $\hat{n} \approx \pm(\mathbf{V}_2 - \mathbf{V}_1)/|\mathbf{V}_2 - \mathbf{V}_1|$. This approximation is valid only for a very high Alfvén Mach number shock (for a very large upstream flow velocity and/or a very small upstream magnetic field intensity). Given this situation, only velocity data are needed to calculate the shock normal vector. This approximation can also be derived from the coupling Rankine-Hugoniot (RH) relations derived by *Chao* [1970], assuming an extremely large Alfvén Mach number [see *Chao*, 1970, section 4.1].

[6] The magnetic field $\mathbf{B}_1$ in the first term on the right hand side of equation (1) can be replaced by $\mathbf{B}_2$ or $\mathbf{B}_2 - \mathbf{B}_1$ [*Abraham-Shrauner and Yun*, 1976]. *Abraham-Shrauner and Yun* [1976] analyzed a variety of mixed data using velocity-magnetic field coplanarity for five interplanetary shocks observed by Pioneer 6 and 7 during the year 1965 to 1966. The estimated shock normal vectors were compared to the previous results obtained by the best estimate and/or average techniques of *Chao* [1970], *Lepping and Argentiero* [1971], and *Dryer et al.* [1972]. They concluded that the mixed data method is useful to obtain an accurate shock normal.

[7] In addition to magnetic field or velocity coplanarity, the RH relations have been used for shock fitting. *Lepping and Argentiero* [1971] used a subset of the isotropic RH relations, including conservation equations for the mass flux, tangential momentum, and normal magnetic field flux to determine the shock frame of reference and the associated parameters ($\mathbf{B}_1$, $\mathbf{B}_2$, $\mathbf{V}_2 - \mathbf{V}_1$, ρ_1, and ρ_2). They employed a least squares method to obtain a best fit solution to these parameters. This work was modified further by *Lepping* [1972] to include the plasma anisotropy in the tangential momentum flux equation. It is found that the shock parameters and the associated shock normal vector are weakly dependent on the anisotropy. However, it can be shown that the magnetic coplanarity theorem is valid for anisotropic plasmas [*Chao*, 1970]. If one applies this theorem to determine the shock normal vector, the vector will not be changed with the anisotropy of the plasmas.

[8] *Viñas and Scudder* [1986] provided a fast and reliable solution for the work of *Lepping and Argentiero* [1971]. *Szabo* [1994] further improved the work of *Viñas and Scudder* [1986]. They adopted a complete set of RH relations. In order to do this, the observed upstream and downstream plasma temperatures should be provided. The improved method was applied to the Neptune bow shock [*Szabo and Lepping*, 1995].

[9] The method of *Viñas and Scudder* [1986] has been applied to the cometary bow shock problem. *Coates et al.* [1990] used this method to fit the bow shock parameters of comet Halley from the Giotto spacecraft data. *Kessel et al.* [1994] further adapted the method of *Viñas and Scudder* [1986] to include the heavy ion effect. They applied both the original single-ion method of *Viñas and Scudder* [1986] and the multiple-ion method to the cometary bow shock, and obtained many bow shock normal vectors after the selection of different data intervals from the upstream (downstream) region. It can be seen that the shock normal vectors produced by the multiple-ion method are within a much smaller angle of each other than those produced by the single-ion method. The multiple-ion model is considered more reliable for cometary bow shock analysis.

[10] The shock normal vector has also been determined using a multiple-spacecraft method. *Chao* [1970] derived an analytical expression for the shock normal vector in terms of the shock contact time, the displacement between two spacecraft and the upstream (downstream) plasma parameters. *Ogilvie and Burlaga* [1969] used a three-spacecraft method to determine the shock normal vector [see also *Lepping and Argentiero*, 1971]. In their method, four equations are needed to solve for the shock propagation speed and the shock normal vector. In addition to the two equations associated with the shock speed in relations to the two spacecraft time delay, the conditions $(\mathbf{B}_2 - \mathbf{B}_1) \cdot \hat{n} = 0$ and $|\hat{n}| = 1$ are also included in the calculation. If one has the relative positions of the associated spacecraft and the shock contact times, the shock normal vector and the associated shock speed can be solved for simultaneously. *Russell et al.* [1983] adopted the method, and used data from the ISEE 1, 2, 3, and IMP 8 spacecraft to determine the shock normal vector of an IP shock.

[11] *Chao and Hsieh* [1984] proposed a method to determine θ_{BN} and M_A, and their estimated errors, without knowing the precise shock normal direction, where θ_{BN} is the angle between the upstream magnetic field and the shock normal and M_A is the upstream Alfvén Mach number. The only measured quantities needed are the plasma density and magnetic fields on both sides of the shock. The present study is a continuation of this method, which generalizes the method to the entire set of the RH relations.

[12] In this paper we propose a new shock fitting procedure to search for an accurate shock frame of reference and the associated parameters with the condition of small alpha particle slippage. The fitting equations we use here are derived from the whole set of conventional and modified RH relations, which do not involve the pressure tensor due to the alpha particle slippage. The modified RH relations include terms for the equivalent "heat flow" and "momentum flux" possibly due to waves/turbulences, energetic particles, and/or other unknown causes [e.g., *Chao and Goldstein*, 1972; *Davison and Krall*, 1977; *Lyu and Kan*, 1986; *Giacalone et al.*, 1997; *Yoon and Lui*, 2006]. Here, a Monte-Carlo calculation method and a minimization technique are used. With this, a best fit solution that satisfies the RH relations is obtained. We test our procedure using several synthetic shocks. The result increases our confidence in our method. A detailed description of our procedure will be given in section 2, while tests of the procedure will be described in section 3. We outline the application of the procedure to IP shocks in section 4. A discussion of the reliability of our procedure will be given in section 5. Finally, in section 6 we discuss the utility of our procedure and the issues of the alpha particle slippage.

2. Procedure

[13] The model is based on the one-fluid anisotropic RH relations. We further separate our procedure under two conditions. In one procedure, we utilize a whole set of the classical RH relations [e.g., *Chao*, 1970] (see Appendix A). It will be called Method A. Another procedure, called Method B, utilizes modified RH relations, which include terms for equivalent "normal momentum flux" and "heat flow" (see Appendix A). These two additional terms are added to the conservation equations for normal momentum and energy flux, respectively [e.g., *Chao and Goldstein*, 1972; *Lyu and Kan*, 1986; *Tsai et al.*, 2002, 2005]. The method is described in detail below.

[14] We have observables: the upstream and downstream magnetic fields ($\mathbf{B}_1$ and $\mathbf{B}_2$), the plasma mass densities (ρ_1 and ρ_2), the plasma anisotropy (ξ_1 and ξ_2), the plasma betas (β_1 and β_2), the difference between the downstream and upstream velocities, $\mathbf{W}$ ($\equiv \mathbf{V}_2 - \mathbf{V}_1$), and the difference between the shock arrival times of the two spacecraft, Δt. Here, $\mathbf{V}$ is defined as the center of mass velocity of the plasmas. The anisotropy parameter is defined as $\xi = 1 - (p_{\parallel} - p_{\perp})/(B^2/\mu_0)$, where $p_{\parallel}$ and $p_{\perp}$ are parallel and perpendicular pressure defined in magnetic field-aligned coordinates, and μ_0 is the magnetic permeability in a vacuum. The plasma beta is defined as $\beta = P/(B^2/(2\mu_0))$, where $P = (p_{\parallel} + 2p_{\perp})/3$ is the thermal pressure of the plasmas. In applications, the upstream and downstream plasma moments have included the contribution from protons, alpha particles, and electrons of solar wind. In general the alpha particles contribute about 4% of the plasma number density in solar wind. The calculations for the plasma moments from the moments of those three particle species will be provided in section 4.1.

[15] The observables defined above are arrays containing observed values in upstream or downstream region. It has an associated mean and error. The total error should consist of an error due to data fluctuation, which is called the sample standard deviation (SD), and a systematic error that may be due to instruments and/or any other uncertainties. The mean and SD are calculated directly from the observable array, and they are the inputs of our procedure. However, the systematic error is usually unknown. In the loss function defined below, it will be given as an additional weight to the SD of the corresponding observable.

2.1. Method A

[16] At the beginning of the procedure, a set of variables is required. These variables include the upstream and downstream magnetic fields, plasma mass densities, and anisotropy parameters. Arrays for these variables are randomly generated, based on the observed means and SDs, by using the Monte-Carlo method [e.g., *Press et al.*, 1992]. The arrays are defined as $\tilde{\mathbf{B}}_1(i)$, $\tilde{\mathbf{B}}_2(i)$, $\tilde{\rho}_1(i)$, $\tilde{\rho}_2(i)$, $\tilde{\xi}_1(i)$, and $\tilde{\xi}_2(i)$, where $i = 1, 2, \ldots, N$. The number N is required to be large in order to have more possibilities available for minimization. In practice, N is at least 10^7 for obtaining a stable solution. Here, each array is generated by using a random number generator function, called $Rnd(\sigma)$. This function generates an array of normally distributed numbers with an average of zero, and the SD calculated from these numbers equals to σ. For example, if the observed (data) mean and SD of the upstream x-component magnetic field are $B_{1x,m}$ and σ_{b1x}, respectively, the array $\tilde{B}_{1x}(i)$ is generated by $\tilde{B}_{1x}(i) = B_{1x,m} + Rnd(\sigma_{b1x})$. Thus the mean and SD of this array equal to $B_{1x,m}$ and σ_{b1x}, respectively.

[17] We use these generated arrays to calculate the derived parameter arrays. The derived parameters are the shock normal vector $\hat{n}$, the shock tangential vector $\hat{t}$, the ratio of downstream to upstream magnetic field intensities m, the ratio of upstream to downstream plasma densities y, the angle, θ_{BN}, of the shock normal with the upstream magnetic field (also called the shock normal angle), and the Alfvén speed V_A. They are calculated via the following equations [*Chao*, 1970]:

$$\hat{n} = \pm \frac{(\mathbf{B}_1 \times \mathbf{B}_2) \times (\mathbf{B}_2 - \mathbf{B}_1)}{|(\mathbf{B}_1 \times \mathbf{B}_2) \times (\mathbf{B}_2 - \mathbf{B}_1)|}, \tag{2}$$

$$\hat{t} = \pm \frac{\mathbf{B}_2 - \mathbf{B}_1}{|\mathbf{B}_2 - \mathbf{B}_1|}, \tag{3}$$

$$m = \frac{B_2}{B_1}, \tag{4}$$

$$y = \frac{\rho_1}{\rho_2}, \tag{5}$$

$$\theta_{BN} = \cos^{-1}(\mathbf{B}_1 \cdot \hat{n}/B_1), \tag{6}$$

$$V_A = \frac{B_1}{\sqrt{\mu_0 \rho_1}}, \tag{7}$$

where equation (2) is known as the magnetic coplanarity theorem. In each derived parameter array, the element with

Table 1. A Summary of the Variables Used in This Procedure

	Method A	Method B
Observables	B_1, B_2, ρ_1, ρ_2, ξ_1, ξ_2, β_1, β_2, $W(\equiv V_2 - V_1)$, Δt	
Variables	$\tilde{\mathbf{B}}_1, \tilde{\mathbf{B}}_2, \tilde{\rho}_1, \tilde{\rho}_2, \tilde{\xi}_1, \tilde{\xi}_2, \tilde{\mathbf{W}}, \Delta\tilde{t}, \tilde{\beta}_1\tilde{\beta}_2$	$\tilde{\mathbf{B}}_1, \tilde{\mathbf{B}}_2, \tilde{\rho}_1, \tilde{\rho}_2, \tilde{\xi}_1, \tilde{\xi}_2, \tilde{\mathbf{W}}, \Delta\tilde{t}, \tilde{\beta}_1, \tilde{\beta}_2$
Derived Parameters	y, m, θ_{BN}, V_A, $\hat{n}$, $\hat{t}$	
Unknowns	(none)	ΔG, ΔQ

index i_0 is calculated from the elements with the same index i_0 in the input variable arrays. For example, $y(i_0) = \tilde{\rho}_1(i_0)/\tilde{\rho}_2(i_0)$. Note that the errors of the input variables will propagate into the derived parameters.

[18] From the RH relations, equations that relate the velocity and plasma beta to the derived parameters can be obtained. These equations are derived in the de Hoffmann-Teller (HT) frame of reference. The equations are expressed as follows (see Appendix A for details).

$$\mathbf{W} = M_{AN} V_A (1-y)\cos\theta_{BN}\hat{n} + M_{AN} V_A (yu-1)\sin\theta_{BN}\hat{t}, \quad (8)$$

$$\beta_2 = \frac{1}{m^2}\left\{\beta_1 - \left\{\left[2\cos^2\theta_{BN}(y-1)\right]M_{AN}^2 + \frac{1}{3}(2\xi_2+1)u^2\sin^2\theta_{BN} - \frac{4}{3}(\xi_2-\xi_1)\cos^2\theta_{BN} - \frac{1}{3}(2\xi_1+1)\sin^2\theta_{BN}\right\}\right\}, \quad (9)$$

$$(1-y)\beta_1 = \left\{\left[\frac{2}{5}\left(u^2\sin^2\theta_{BN} - 4\cos^2\theta_{BN}\right)\right]y^2 + 2\cos^2\theta_{BN}y - \frac{2}{5}\right\}\cdot M_{AN}^2 + \left[\frac{1}{5}(1-6\xi_2)u^2\sin^2\theta_{BN} + \frac{4}{15}(3\xi_2 - 5\xi_1 + 2)\cdot\cos^2\theta_{BN} + \frac{1}{3}(2\xi_1+1)\sin^2\theta_{BN}\right]y + \frac{8}{15}(\xi_1 - 1), \quad (10)$$

$$M_{AN} \equiv \frac{V_{n1}^*}{V_A\cos\theta_{BN}} = \left(\frac{\xi_2 u - \xi_1}{yu-1}\right)^{1/2}, \quad (11)$$

where M_{AN} is the upstream normal Alfvén Mach number, and V_{n1}^* is the upstream normal flow speed in the HT frame of reference. Moreover,

$$u \equiv \frac{B_{t2}}{B_{t1}} = \left(\frac{m^2 - \cos^2\theta_{BN}}{\sin^2\theta_{BN}}\right)^{1/2} \quad (12)$$

is the ratio of the upstream to downstream tangential magnetic fields. Note that there is a condition of no solution for M_{AN} in equation (11) as $(\xi_2 u - \xi_1)/(yu - 1) < 0$. Moreover, for anisotropic case, if $M_{AN} < (\xi_1)^{1/2}$, the solution is not a fast shock (see equation (B2) in Appendix B). Our procedure eliminates those samples under these two conditions from the operated arrays.

[19] The RH relations used in our model do not involve the effect due to alpha particle slippage relative to protons (see Appendix A and also Appendix D). Here we assume that the slippage pressure tensor is unimportant; thus the procedure can only be applied to the cases of ignorable slippage pressure tensor. From the WIND observations near the ecliptic plane, we found that in general the effect of alpha particle slippage to the RH relations is ignorable for interplanetary shocks, which supports this approximation. Therefore we suggest that our procedure can be applied to most interplanetary shocks observed near the ecliptic plane. However, if the slippage is large, the magnetic coplanarity theorem (i.e., equation (2)) is not valid any more, and the shock normal array cannot be calculated with our procedure. In addition, $[V_q] = 0$ in the RH relations (see Appendix A) is not valid as well. Expression (8) cannot be derived. Thus in such a case our procedure cannot be applied. The associated issues will be further discussed in section 6.

[20] The local shock propagation speed in spacecraft frame of reference can be calculated as $V_s = M_A V_A + \mathbf{V}_1 \cdot \hat{n}$, where $M_A \equiv V_{n1}^*/V_A$ is the Alfvén Mach number, and $\mathbf{V}_1$ is the center of mass velocity of the plasmas in upstream region. The Alfvén Mach number can also be calculated via $M_A = M_{AN}\cos\theta_{BN}$. From the geometry of two spacecraft observations, the time difference between two observations can be calculated by

$$\Delta t = \frac{\Delta\mathbf{R}\cdot\hat{n}}{V_s} = \frac{\Delta\mathbf{R}\cdot\hat{n}}{M_A V_A + \mathbf{V}_1\cdot\hat{n}}, \quad (13)$$

where $\Delta\mathbf{R}$ is the vector displacement of the two spacecraft. The expression is valid given the assumption that the planar shock propagates at a constant shock speed between the two spacecraft. When the values in parameter arrays $m(i)$, $y(i)$, $\theta_{BN}(i)$, $V_A(i)$, $\hat{n}(i)$, $\hat{t}(i)$, $\tilde{\xi}_1$ (i), and $\tilde{\xi}_2$ (i), and values for $\Delta\mathbf{R}$ and $\mathbf{V}_1$ are put into equations (8)–(13), the values of the variable arrays $\tilde{\mathbf{W}}(i)$, $\Delta\tilde{t}(i)$, $\tilde{\beta}_1$ (i), and $\tilde{\beta}_2$ (i) can thus be obtained. The variables used in Method A are summarized in Table 1.

[21] Now we have 16 arrays for all the variables. A so-called loss function, which measures how well the variables can fit the observed means, is defined here. The best estimate of the variables is defined to be the value that minimizes the loss function. The loss function is defined as

$$L(i) \equiv \sum_{k=1}^{16}\left[\frac{X_k(i) - \langle Y_k\rangle}{\sigma_k}\right]^2, \quad (14)$$

where $X_k(i) \equiv (\tilde{B}_{1x}(i), \tilde{B}_{1y}(i), \tilde{B}_{1z}(i), \tilde{B}_{2x}(i), \tilde{B}_{2y}(i), \tilde{B}_{2z}(i), \tilde{\rho}_1(i), \tilde{\rho}_2(i), \tilde{\xi}_1(i), \tilde{\xi}_2(i), \tilde{\beta}_1(i), \tilde{\beta}_2(i), \tilde{W}_x(i), \tilde{W}_y(i), \tilde{W}_z(i), \Delta\tilde{t}(i))$ represents the arrays of the variables where the index i runs from 1 to a large number N, and the $\langle Y_k\rangle$ is the mean of each observable $Y_k(j)$, where $Y_k(j) \equiv (B_{1x}(j), B_{1y}(j), B_{1z}(j), B_{2x}(j), B_{2y}(j), B_{2z}(j), \rho_1(j), \rho_2(j), \xi_1(i), \xi_2(i), \beta_1(j), \beta_2(j), W_x(j), W_y(j), W_z(j), \Delta t(j))$ represents the arrays of the observables. Here the index j runs from 1 to M_k, where M_k represents the number of data points of the kth observable. The error σ_k is defined as the sum of the SD and the systematic errors,

$$\sigma_k = \sigma_k' + \sigma_k'', \quad (15)$$

where

$$\sigma_k' \equiv \left[\frac{\sum_{j=1}^{M_k}\left(Y_k(j)-\langle Y_k\rangle\right)^2}{M_k-1}\right]^{1/2}, \tag{16}$$

is the data SD, and σ_k'' represents the systematic error of the kth observable. In application, we often do not know the magnitude of the systematic error in the data, thus $\sigma_k'' = (1/2)\sigma_k'$ is assumed for all the analyzed cases in this study.

2.2. Method B

[22] The major difference of Method B from Method A is to introduce terms for an equivalent "normal momentum flux" and "heat flow" in the RH relations. In this model, two addition parameters, ΔG and ΔQ, are derived from those two terms in the RH relations (for details, see Appendix A). In applying to shocks, we first use Method A to test if the parameters are fitted well without these excess amounts. In some interplanetary shocks, the shock parameters are not fitted well. Sometimes the best fit plasma betas deviate more than 2 SDs from their observed means. In such a condition, we try the Method B instead. With Method B, we are able to estimate the amounts of the ΔG and ΔQ.

[23] In Method B, the arrays $\tilde{\mathbf{B}}_1(i)$, $\tilde{\mathbf{B}}_2(i)$, $\tilde{\rho}_1(i)$, $\tilde{\rho}_2(i)$, $\tilde{\xi}_1$ (i), $\tilde{\xi}_2$ (i), $\tilde{\beta}_1$ (i), and $\tilde{\beta}_2$ (i) are randomly generated by using the same random number generator function, $Rnd(\sigma)$, used in Method A. After that, the derived parameter arrays are calculated also via equations (2)–(7). The calculations are the same as in Method A.

[24] The introducing of ΔG and ΔQ leads to changes in equations (9) and (10). The modified equations are as follows (for details, see Appendix A):

$$\begin{aligned}\beta_2 = \frac{1}{m^2}\{\beta_1 - \{[(2\cos^2\theta_{BN})y + 2(\Delta G-1)\cos^2\theta_{BN}]M_{AN}^2 \\ + \frac{1}{3}(2\xi_2+1)u^2\sin^2\theta_{BN} - \frac{4}{3}(\xi_2-\xi_1)\cos^2\theta_{BN} \\ - \frac{1}{3}(2\xi_1+1)\sin^2\theta_{BN}\}\},\end{aligned} \tag{9'}$$

$$\begin{aligned}(1-y)\beta_1 = \left\{\left[\frac{2}{5}\left(u^2\sin^2\theta_{BN} - 4\cos^2\theta_{BN}\right)\right]y^2 \right. \\ \left. + \left[2(1-\Delta G)\cos^2\theta_{BN}\right]y + \frac{2}{5}\left(\Delta Q\cos^2\theta_{BN} - 1\right)\right\} \\ \cdot M_{AN}^2 + \left[\frac{1}{5}(1-6\xi_2)u^2\sin^2\theta_{BN} + \frac{4}{15}\right. \\ \left.\cdot(3\xi_2 - 5\xi_1 + 2)\cos^2\theta_{BN} + \frac{1}{3}(2\xi_1+1)\sin^2\theta_{BN}\right]y \\ + \frac{8}{15}(\xi_1-1),\end{aligned} \tag{10'}$$

where ΔQ and ΔG are defined as

$$\Delta Q \equiv \frac{q_{2n} - q_{1n}}{(1/2)\rho_1 V_{1n}^{*3}}, \tag{17}$$

$$\Delta G \equiv \frac{g_{2n} - g_{1n}}{\rho_1 V_{1n}^{*2}}. \tag{18}$$

Here, q_{1n} (q_{2n}) and g_{1n} (g_{2n}) represent the equivalent "heat flow" and "momentum flux" in the normal direction on the upstream (downstream) side of a shock. In principle, equations (9′) and (10′) can be expressed as two equations: $h_1(\Delta G, \Delta Q) = f_1$ $(y, u, \theta_{BN}, \beta_1, \beta_2, \xi_1, \xi_2)$ and $h_2(\Delta G, \Delta Q) = f_2$ $(y, u, \theta_{BN}, \beta_1, \beta_2, \xi_1, \xi_2)$. As we have the upstream and downstream magnetic fields, plasma densities, plasma betas, and the anisotropy parameters, the ΔG and ΔQ can be evaluated. Therefore as the values in parameter arrays $m(i)$, $y(i)$, $\theta_{BN}(i)$, $V_A(i)$, $\hat{n}(i)$, $\hat{t}(i)$, $\tilde{\xi}_1$ (i), $\tilde{\xi}_2$ (i), $\tilde{\beta}_1$ (i), and $\tilde{\beta}_2$ (i), and values for $\Delta\mathbf{R}$ and $\mathbf{V}_1$ are put into equations (8), (9′), (10′), and (11)–(13), the values of the arrays $\tilde{\mathbf{W}}(i)$, $\Delta\tilde{t}(i)$, as well as $\Delta G(i)$ and $\Delta Q(i)$ can thus be obtained. The variables used here are also tabulated in Table 1.

[25] After we have arrays for all the variables, we use the same loss function defined in equation (14) for the minimization technique. Note that here the $\Delta G(i)$ and $\Delta Q(i)$ are not included in this loss function, since we do not have the observed values for them. The solution for ΔG and ΔQ are simultaneously obtained when the best fit solution for the other variables are found. In our minimization in Method B, it is easy to understand that the best fit solution of β_1 and β_2 always fall to their means due to the two degrees of freedom provided by ΔG and ΔQ. The associated issue will be discussed in section 3.1 and section 5.

3. Fitting With Synthetic Shocks

[26] Several synthetic shocks are used to test our procedure. The first one is an oblique shock where the equivalent "heat flow" and "momentum flux" are not needed. The second oblique shock does need such additional quantities. We also use an exactly perpendicular shock, a shock with $\theta_{BN} = 89°$, and a shock with $\theta_{BN} = 1°$ to test our method. In application, we first investigate whether the model without "heat flow" and "momentum flux" can be applied to a shock by using Method A. Then, we use Method B to analyze shocks when the equivalent "heat flow" and "momentum flux" are needed.

3.1. An Oblique Shock Without ΔG and ΔQ

[27] We manufacture shock structures for a synthetic oblique fast shock that requires neither ΔG nor ΔQ. The associated shock parameters are listed in Table 2. These parameters are solutions of the RH relations. Once the values of the magnetic field, plasma density, anisotropy parameter, plasma beta, and upstream velocity are given, the other parameters can be calculated. Here, an equivalent proton number density, N_{eq}, is defined as $N_{eq} \equiv \rho/m_p$, where $m_p = 1.6726 \times 10^{-27}$ kg is the proton mass. On the other hand, the local shock speed and hence the time difference between two spacecraft observations can be calculated from the associated shock parameters via equation (13). We assume that this shock has been observed by two spacecraft at different locations at a time delay, Δt. The two observations are set to have a spatial displacement of $(-100, 100, 0)$ R_E; hence the calculated time difference is 21.5 min. Here the GSE coordinate system is used, and the R_E is the Earth radius equaling to 6378 km.

[28] The values listed in Table 2 are called the "true answer." The plasmas on both sides of the shock are assumed to be isotropic (i.e., $\xi_1 = 1$ and $\xi_2 = 1$). The

Table 2. "True Answer" of the First Synthetic Shock

Parameter	Value
Magnetic field $\mathbf{B}_1$, $\mathbf{B}_2$, [a] nT	(−6.1, −0.52, −7.8), (−7.0, −0.79, −10.9)
Plasma density N_{eq1}, N_{eq2}, [b] cm^{-3}	8.2, 10.8
Plasma beta β_1, β_2	0.272, 0.260
Anisotropy parameter ξ_1, ξ_2	1.0, 1.0
Density ratio y	0.759
Magnetic field intensity ratio m	1.309
Shock normal angle θ_{BN}, deg	68.1
Upstream Alfvén speed V_A, km/s	75.5
Shock normal vector $\hat{n}$	(−0.960, 0.067, 0.273)
Tangential magnetic field ratio u	1.352
Tangential velocity ratio $z = yu$	1.027
Mach numbers M_A, M_{AN}, M_{AN2}, M_F, M_{F2}	1.35, 3.64, 3.18, 1.24, 0.82
Heat flow and normal momentum ΔG, ΔQ	0, 0
Flow velocities $\mathbf{V}_1$, $\mathbf{V}_2$, km/s	(−430.0, 10.0, −30.0), (−451.8, 12.2, −16.8)
Velocity difference $\mathbf{W}$, km/s	(−21.79, 2.22, 13.21)
Shock speed versus, km/s	507.6
Spacecraft displacement $\Delta\mathbf{R}$, R_E	(−100.0, 100.0, 0.0)
Time difference Δt, min	21.50

[a]It is assumed here that GSE coordinate system is used.
[b]The plasma number density, N_{eq}, is defined as $N_{eq} = \rho/m_p$, where $m_p = 1.6726 \times 10^{-27}$kg is proton mass.

downstream normal Alfvén Mach number M_{AN2} and the upstream and downstream fast Mach numbers M_F and M_{F2} can be calculated in terms of the derived parameters. They are expressed as (see Appendix B)

$$M_{AN2} = M_{AN}\sqrt{y}, \tag{19}$$

$$M_F = \left[\frac{2M_{AN}^2\cos^2\theta_{BN}}{(1+\gamma\beta_1/2)+\left[(1+\gamma\beta_1/2)^2-2\gamma\beta_1\cos^2\theta_{BN}\right]^{1/2}}\right]^{1/2}, \tag{20}$$

$$M_{F2} = \left[\frac{2M_{AN2}^2\cos^2\theta_{BN}/m^2}{(1+\gamma\beta_2/2)+\left[(1+\gamma\beta_2/2)^2-2\gamma\beta_2\cos^2\theta_{BN}/m^2\right]^{1/2}}\right]^{1/2}, \tag{21}$$

where $\gamma = 5/3$ is used. We also show the parameter z ($\equiv V_{t2}^*/V_{t1}^* = yu$) in Table 2 (see also equations (A11)–(A13) in Appendix A). It is an important parameter to determine whether the solution for the Alfvén Mach number M_{AN} in equation (11) is real.

[29] Now, we assume that we have the data set of a shock. Figure 1 shows the simulated data for the magnetic field and the plasma moments. As can be seen, the shock layer is between $t = 6$ and $t = 7$ min. Since we do not have the data fluctuation spectrum model, for simplicity the values on both sides of the shock are assumed to have a normal distribution. Thus the values are also generated by using the same random number generator function, $Rnd(\sigma)$, defined in section 2. The data on the shock layer that connects the two sides are made using a hyperbolic tangent function, upon which some random values are added, so the shock layer does not look smooth. Note that the magnetic field and plasma data within the shock layer are not used here in our analysis.

[30] In order to give reasonable error sizes for each observable, we estimate errors using observations from real IP shocks. From 61 IP shocks observed by WIND during the period from 1995 to 2000, the average values of the ratios of the sample error to the magnitude of the shock jump for the magnetic field, plasma density, and the velocity are estimated to be ~0.1. According to these estimates, the error for each component of the magnetic field, in this simulation, is set to be 0.3 nT. The error for the plasma density is set to be 0.26 (proton mass/cm^3). The error for the velocity is set to be 2 km/s. For the plasma betas, the ratio of the error to the average of the observed magnitude $(\beta_1+\beta_2)/2$ is estimated on an average to be ~0.1. Thus the error for the plasma betas, in this simulation, is set to be about 0.027. Moreover, for the anisotropy parameters, the ratio of the error to the average of the observed magnitude is estimated on an average to be ~0.04. Thus the error for the anisotropy parameters is set to be about 0.04.

[31] In an attempt to simulate the presence of a systematic error in addition to the sample SD, the data of the magnetic field, plasma density, and anisotropy parameter are randomly shifted so that their means do not coincide with the "true answer." This error cannot be known from data sampling. It comes from an error in measurements caused by any mechanism. The magnitudes of the shifts are within 1/2 data sample SD.

[32] As can be seen in Figure 1, the vertical lines indicate the time intervals of the up- and downstream data selected for the observables. The upstream is from t_1 to t_2 (from 1 to 6 min), and the downstream is from t_3 to t_4 (from 7 to 12 min). The SD (σ') for each observable is calculated from the data fluctuations via equation (16). Figure 2 shows the magnetic field and plasma moments of the selected intervals. The dot and error bar indicate the mean and SD, respectively, for the selected interval. Moreover, the dotted line indicates the value of the "true answer." As can be seen, the data means for the magnetic fields, plasma densities, and anisotropy parameters have some biases from the "true answer." These asymmetric biases represent the systematic errors.

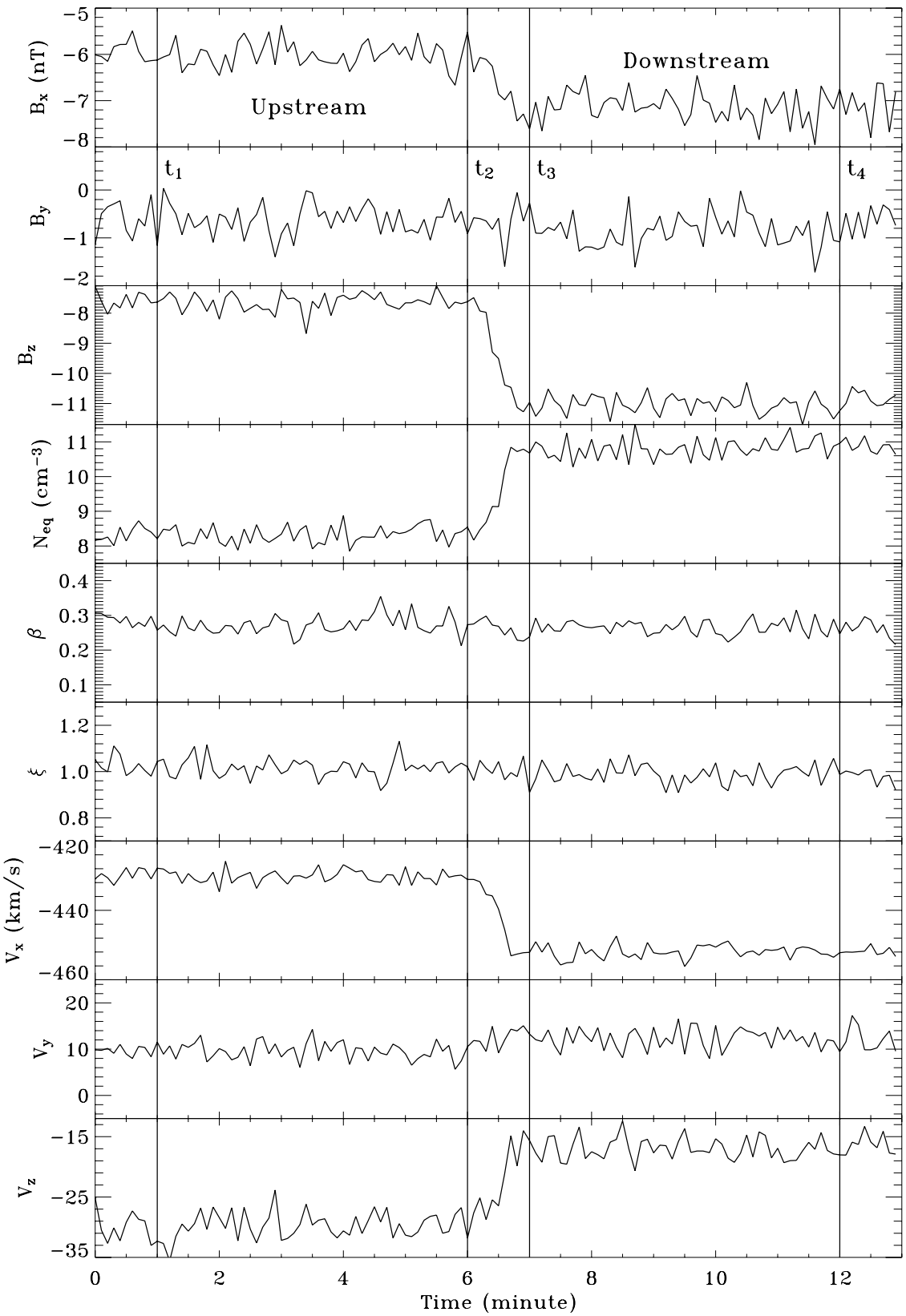

Figure 1. The simulated data for the first synthetic shock: From up to bottom are the magnetic field, plasma density, anisotropy parameter, plasma beta, and velocity. It is assumed that GSE coordinate system is used. $N_{eq} = \rho/m_p$, is defined as the equivalent proton number density, where m_p is the proton mass. The vertical lines indicate the data interval for the upstream (t_1–t_2) and downstream (t_3–t_4) sides. The shock layer is between $t = 6$ and $t = 7$ min.

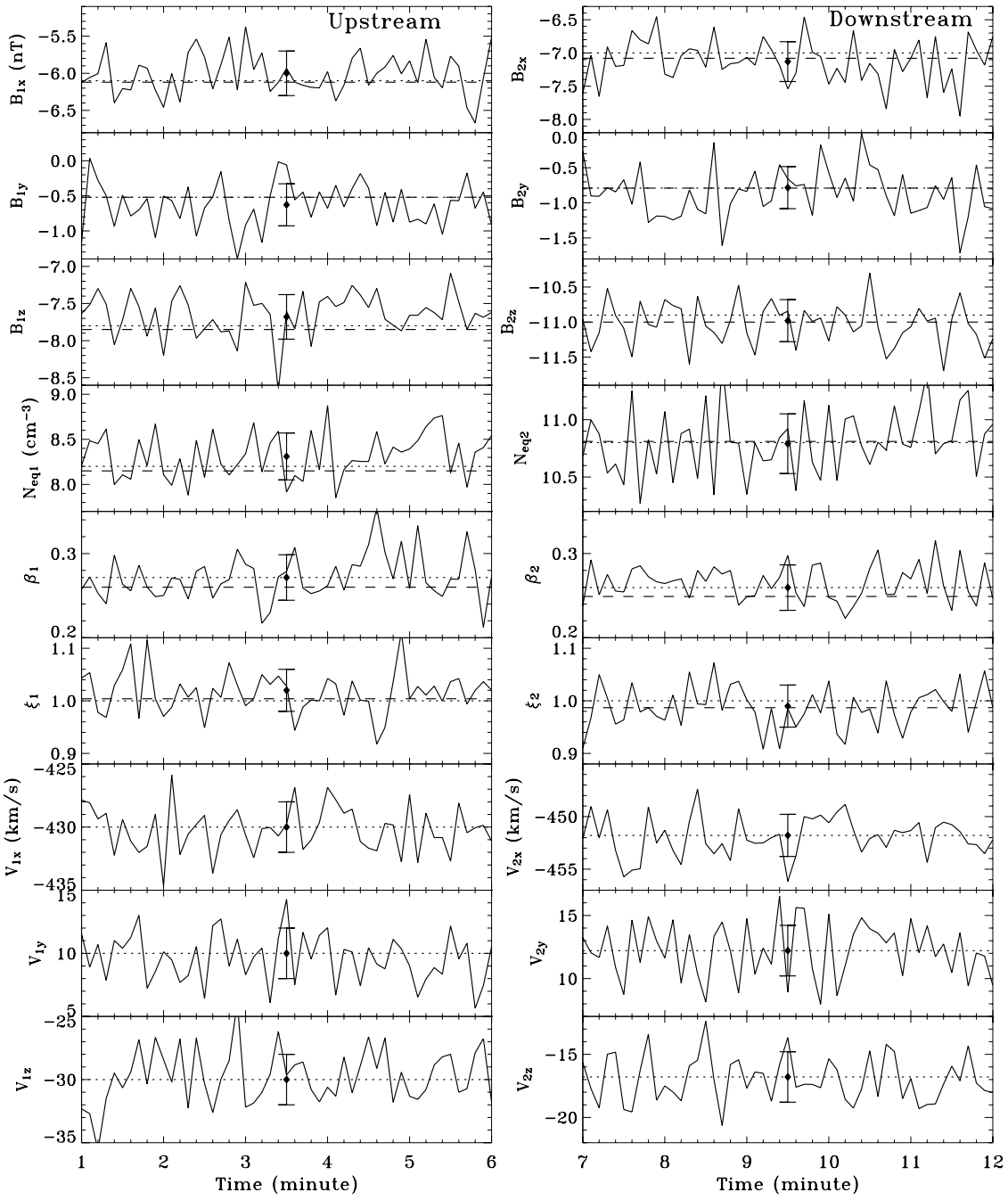

Figure 2. The magnetic field and plasma moment data selected from the simulated data. The plots on the left side are for the upstream (t_1–t_2), and on the right side are for the downstream (t_3–t_4). The error bars indicate the data means and SDs, while the dotted lines indicate the "true answer" values. On the other hand, the dashed lines indicate the best fit values from our procedure.

[33] The associated mean and SD of the observables are listed in Table 3. For the error of **W**, an effective sample deviation is calculated from the upstream and downstream velocities via the Monte-Carlo method. First, two arrays of $\mathbf{V}_1(j)$ and $\mathbf{V}_2(j)$ are randomly generated, using the function $Rnd(\sigma)$, based on the means and SDs of the observed upstream and downstream velocities. The array of **W** is defined as

$$\mathbf{W}(j) = \mathbf{V}_2(j) - \mathbf{V}_1(j) \tag{22}$$

Then the mean and error are calculated directly from this array. The estimated error of **W** for the present case is ~2.8 km/s.

[34] The difference of the shock arrival times, Δt, is also given in Table 3. The uncertainty of Δt comes from that of the second spacecraft. The magnitude of the error depends on the time resolution of the data and the thickness of the shock layer. We assume that the shock is observed by two spacecraft at two different locations, with a time delay $\langle \Delta t \rangle$ = 21.5 min and a spatial displacement of $\Delta\mathbf{R}$ = (−100,

Table 3. Means and SDs of the First Synthetic Shock

Observable	Mean	Standard Deviation
$\mathbf{B}_1$, nT	(−6.00, −0.628, −7.68)	0.3
$\mathbf{B}_2$	(−7.13, −0.783, −10.98)	0.3
N_{eq1}, cm^{-3}	8.31	0.26
N_{eq2}	10.79	0.26
ξ_1	1.02	0.04
ξ_2	0.99	0.04
β_1	0.272	0.027
β_2	0.260	0.027
$\mathbf{W}$, km/s	(−21.79, 2.22, 13.21)	2.8
Δt, min	21.50	0.1

100, 0) R_E (in GSE). The uncertainty of Δt is set to be 0.1 min. No uncertainty about the spacecraft positions is given.

[35] First we apply Method A to this case. According to the means and SDs of the observables shown in Table 3, ten arrays for the variables $\tilde{\mathbf{B}}_1(i)$, $\tilde{\mathbf{B}}_2(i)$, $\tilde{\rho}_1(i)$, $\tilde{\rho}_2(i)$, $\tilde{\xi}_1(i)$, and $\tilde{\xi}_2(i)$ are generated. Here the function $Rnd(\sigma)$ defined in section 2 is used. The mean and SD of the upstream x-component magnetic field are measured to be $B_{1x,mean} = -6.0$ and $\sigma'_{B1x} = 0.3$ nT, while the array $\tilde{B}_{1x}(i)$ are generated by $\tilde{B}_{1x}(i) = B_{1x,mean} + Rnd(\sigma'_{B1x})$. Thus the array has normally distributed values, for which the mean and SD equal to −6.0 and 0.3 nT, respectively. The operation is the same for all the other variable arrays.

[36] Using equations (2)–(7), we derive the parameters $\hat{n}(i)$, $\hat{t}(i)$, $m(i)$, $y(i)$, $\theta_{BN}(i)$, and $V_A(i)$, from those generated arrays. The corresponding means and errors of the parameters are listed in Table 4. The shock normal is calculated directly from the means of the observables via equation (2). It is about 8° off from the "true answer." We show the error cone angles of the shock normal and tangential vectors in Table 4. Here the error cone angle is defined to be $Max(\cos^{-1}(\hat{n}(i)\cdot\bar{\hat{n}}))$, where $\bar{\hat{n}}$ is calculated from the means of the observables.

[37] Table 4 also shows the corresponding velocity difference $\mathbf{W}$, plasma betas, and the Mach numbers calculated directly from the data means via equations (2)–(12) and (19)–(21). They have a large discrepancy from the "true answer." The value of the upstream fast Mach number turns out to be less than 1, which is not permissible for a fast shock. Thus the shock parameters calculated directly from these measured means do not necessarily satisfy the shock jump relations.

[38] With the derived parameter arrays, the variables $\tilde{\mathbf{W}}(i)$, $\Delta\tilde{t}(i)$, $\tilde{\beta}_1(i)$, and $\tilde{\beta}_2(i)$ are calculated via equations (8)–(13). Figure 3 shows distributions of the values for the arrays for the parameters calculated from the magnetic field, plasma density, and anisotropy parameter. The shock normal is shown by a polar-angle representation, ϕ and θ. The property in equation (11) shows that as $(\xi_2 u - \xi_1)/(yu - 1) < 0$, M_{AN} has no solution. Moreover, if $M_{AN} < (\xi_1)^{1/2}$, the solution is not a fast shock. The elements of M_{AN}, $\tilde{\mathbf{W}}$, $\tilde{\beta}_1$, $\tilde{\beta}_2$, and $\Delta\tilde{t}$ under these two conditions have been checked and eliminated by our program. For the present case, about 12% of the total elements are eliminated. For an array size of $N = 10^7$, about 9×10^6 samples remain to be useful to calculate the values of $\tilde{\mathbf{W}}(i)$, $\tilde{\beta}_1(i)$, $\tilde{\beta}_2(i)$, and $\Delta\tilde{t}(i)$.

[39] Now we have 16 arrays for all the variables. With the 16 variable arrays as well as the 16 observable arrays, the loss function defined in equation (14) can be calculated. On the other hand, for calculating the loss function, the systematic error in equation (15) is assumed to be $\sigma''_k = (1/2)\sigma'_k$ for all the variables. Now the values of the array of loss function $L(i)$ are obtained, and the best fit solution is the one with a minimum $L(i)$. A best fit solution is thus found and the result is listed in Table 5 (Method A). In comparison with Table 2, it is found that the results are very close to the "true answer." The shock normal obtained from this method is (−0.957, 0.068, 0.281) which is only ∼0.5° off from the "true answer." Moreover, the estimated values for the Mach numbers and the shock speed are also comparable to the "true answer." The best fit values of the magnetic fields, plasma densities, plasma betas, and the anisotropy parameters are indicated in Figure 2 (dashed lines). As can be seen, the best fit values are close to the "true answer" values (dotted lines). For the plasma velocity, we only have the best fit value of $\mathbf{W}$, instead of $\mathbf{V}_1$ and $\mathbf{V}_2$. Thus it is not shown in this figure. However, as can be seen in Table 5, the best fit value of $\mathbf{W}$ is very close to the "true answer."

[40] Now we apply Method B to the same shock. Here, the plasma betas are treated as inputs. From the data means and SDs shown in Table 3, 12 arrays $\tilde{\mathbf{B}}_1(i)$, $\tilde{\mathbf{B}}_2(i)$, $\tilde{\rho}_1(i)$, $\tilde{\rho}_2(i)$, $\tilde{\xi}_1(i)$, $\tilde{\xi}_2(i)$, $\tilde{\beta}_1(i)$, and $\tilde{\beta}_2(i)$ are generated. The same random generator function is utilized here. Also using

Table 4. Values of the Derived Parameters From the Data of the First Synthetic Shock

Parameter	Mean	Deviation	Error Cone Angle, deg
y	0.770	0.03	
m	1.342	0.05	
θ_{BN}	70.8	7.7	
V_A	73.9	2.6	
$\hat{n}$	(−0.943, −0.068, 0.325)		∼63
$\hat{n}$	(0.323, 0.044, 0.945)		∼27
	Parameters Calculated From Data Means (Method A)		
$\mathbf{W}$, km/s	(−9.24, −0.45, 14.10)		
β_1, β_2	−0.94, −0.80		
M_A, M_{AN}, M_{AN2}, M_F, M_{F2}	0.79, 2.40, 2.11, 0.72, 0.47		
	Parameters Calculate From Data Means (Method B)		
$\mathbf{W}$, km/s	(−9.24, −0.45, 14.10)		
ΔG, ΔQ	−0.56, −1.06		
M_A, M_{AN}, M_{AN2}, M_F, M_{F2}	0.79, 2.40, 2.11, 0.72, 0.47		

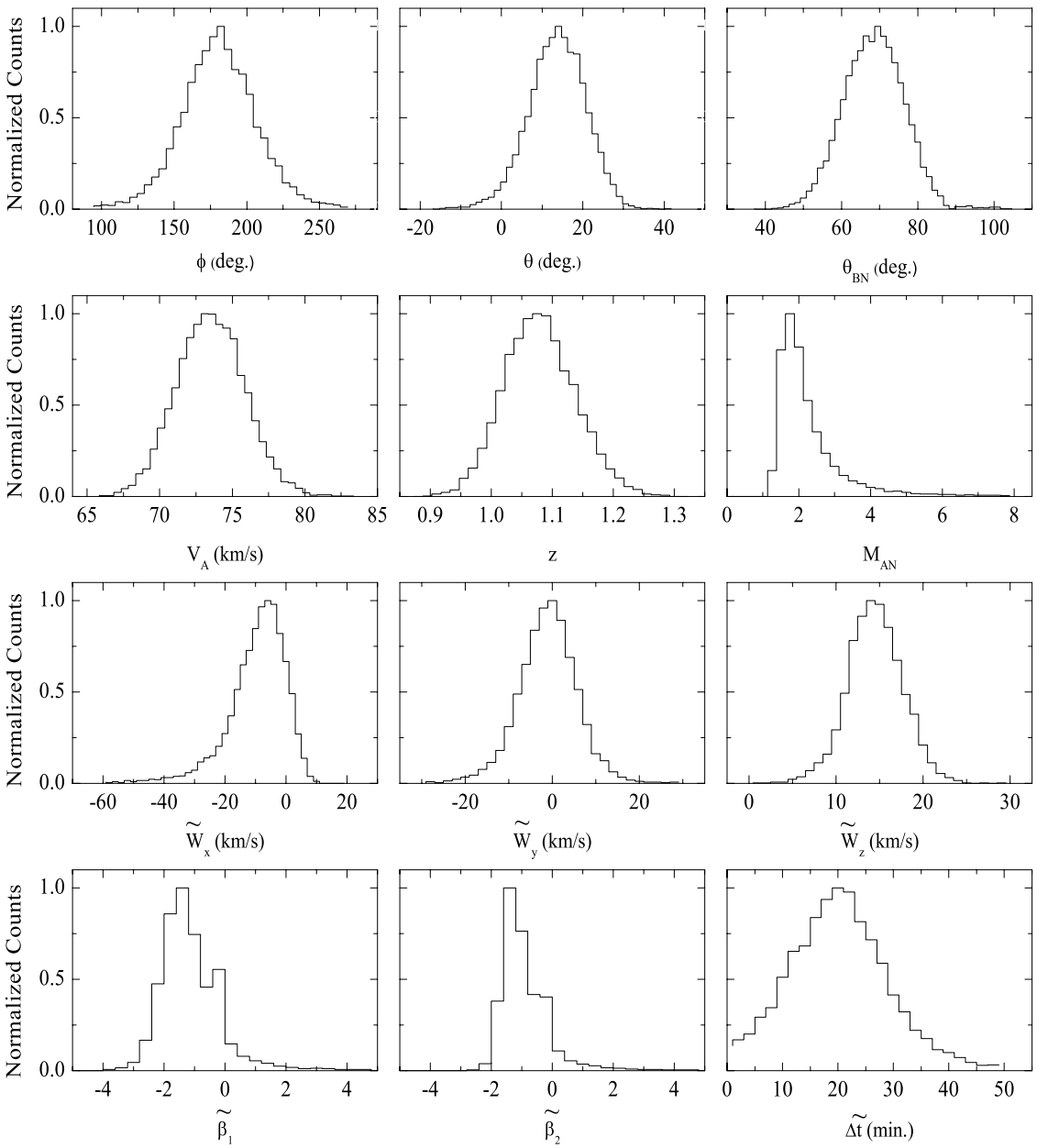

Figure 3. The distributions of the arrays: The y axis shows the numbers normalized by the maximum count. The first two plots in the upper line show the polar angles (ϕ, θ) of the shock normal vector.

equations (2)–(7), we have the derived parameter arrays from those variables.

[41] Via equation (8), the corresponding velocity difference **W** is calculated from the data means of the magnetic field, plasma density, and anisotropy. The result is shown in Table 4 (Method B). The Mach numbers calculated from the data means via equations (11) and (19)–(21) are also shown in Table 4. Equations (9′) and (10′) are used to calculate the ΔG and ΔQ, from the data means of the magnetic field, plasma density, plasma beta, and anisotropy. The result is also shown in Table 4. As can be seen, these calculated values have a large discrepancy from the "true answer."

[42] With the derived parameters, the variables $\tilde{\mathbf{W}}(i)$, $\Delta\tilde{t}(i)$, $\Delta G(i)$ and $\Delta Q(i)$ are calculated via equations (2)–(8), (9′), (10′), and (11)–(13). Now we have 18 arrays, in which the $\Delta G(i)$ and $\Delta Q(i)$ are not included in the loss function. A best fit solution is found using the same minimization method and the result is listed in Table 5 (Method B). It is found that the results from Method A and Method B are very close to each other, and they agree well with the "true answer." The shock normal obtained from Method B is $(-0.959, 0.057, 0.278)$ which is only $\sim 0.6^\circ$ off from the "true answer" shock normal. Moreover, the estimated values for the Mach numbers and the shock speed are also comparable to the "true answer."

[43] The solutions of ΔG and ΔQ cannot be found by using the loss function, since there is no observed value for them. They provide two degrees of freedom. The values of them are estimated by the other parameters via equations (9′) and (10′). The parameters y, m, θ_{BN}, and $\hat{n}$ can be fitted

Table 5. Best Fit Solutions Estimated From Method A and Method B for the First Synthetic Shock

Parameter	Method A	Method B
$\mathbf{B}_1$, nT	(−6.13, −0.52, −7.85),	(−6.14, −0.63, −7.79),
$\mathbf{B}_2$	(−7.08, −0.79, −11.03)	(−7.09, −0.94, −11.00)
N_{eq1}, N_{eq2}, cm^{-3}	8.15, 10.81	8.16, 10.85
ξ_1, ξ_2	1.00, 0.99	1.01, 0.99
β_1, β_2	0.26, 0.25	0.27, 0.26
y	0.755	0.752
m	1.316	1.320
θ_{BN}, deg	68.7	68.2
V_A, km/s	76.2	75.9
$\hat{n}$	(−0.957, 0.068, 0.281)	(−0.959, 0.057, 0.278)
u	1.358	1.365
z (=yu)	1.024	1.026
M_A, M_{AN}, M_{AN2}, M_F, M_{F2}	1.35, 3.70, 3.22, 1.23, 0.81	1.34, 3.62, 3.13, 1.22, 0.80
ΔG, ΔQ	0, 0	-0.005 ± 0.008, -0.01 ± 0.03[a]
$\mathbf{W}$, km/s	(−22.2, 2.2, 13.2)	(−22.3, 2.0, 13.4)
V_s, km/s	506.4	506.2
Δt, min	21.5	21.3

[a]The uncertainties of ΔG and ΔQ shown in the best fit result come from the uncertainties of the plasma betas.

well by virtue of equations (2)–(8), (11)–(13), and the loss function, and their confidence regions are very small. Unlike in Method A, the β_1 and β_2 in Method B are not fitted due to the two degrees of freedom. They are only estimated by the minimization of the loss function. Thus the best fit solutions for β_1 and β_2 should equal to their data means. However, the data of β_1 and β_2 also have uncertainties that will propagate to ΔG and ΔQ. These uncertainties should be taken into account.

[44] In principle, the uncertainties of parameters other than the plasma betas should also propagate to ΔG and ΔQ. However, the confidence region of the other parameters is small; thus only small amounts of uncertainties actually propagate to ΔG and ΔQ. Therefore the uncertainties of ΔG and ΔQ are dominated by that of β_1 and β_2. If we want to estimate the uncertainty by all the other parameters, one method is that we repeat the procedure several times, for example, 10 times, and estimate the sample SDs of those resultant ΔGs and ΔQs. The SDs can be considered as the uncertainties of the ΔG and ΔQ in addition to the uncertainties shown in Table 5.

[45] The uncertainties of β_1 and β_2 also propagate into the fast Mach numbers via equations (20) and (21). The method for determining the uncertainties of ΔG, ΔQ, and the fast Mach numbers will be given further in section 5. The results of Method B show that both ΔG and ΔQ are small enough that within the uncertainty, they can be considered to vanish. Therefore we demonstrate that Method A and Method B of our procedure is capable of finding the correct parameters of a shock when ΔG and ΔQ are not needed in the RH relations.

3.2. An Oblique Shock Requiring ΔG and ΔQ

[46] Now we apply our procedure to another synthetic oblique shock with a significant amount of ΔG (=0.22) and ΔQ (=0.79). The "true answer" for the synthetic shock is listed in Table 6. Here, we also make a data shift of ~1/2 SD from the "true answer" for the magnetic field, plasma density, and anisotropy parameter. So, the data means do not coincide with the values of the "true answer." On the other hand, the shock is assumed to be observed by two spacecraft with a displacement of (−100, 100, 0) R_E (GSE); therefore the time delay can be obtained to be 28.45 min.

Table 6. "True Answer" and the Best Fit Values of the Second Synthetic Shock

Parameter	"True Answer" Value	Best Fit Value
$\mathbf{B}_1$, nT	(−1.9, 1.6, 0.35),	(−1.92, 1.60, 0.29),
$\mathbf{B}_2$, nT	(−2.3, 3.0, 1.1)	(−2.30, 3.04, 1.01)
N_{eq1}, N_{eq2}, cm^{-3}	19.0, 33.5	19.0, 33.8
ξ_1, ξ_2	1.00, 1.00	0.99, 1.01
β_1, β_2	5.0, 3.0	5.0, 3.0
y	0.567	0.563
m	1.569	1.570
θ_{BN}, deg	52.6	51.4
V_A, km/s	12.6	12.6
$\hat{n}$	(−0.927, −0.067, −0.369)	(−0.931, −0.070, −0.359)
u	1.823	1.843
z (=yu)	1.034	1.040
M_A, M_{AN}, M_{AN2}, M_F, M_{F2}	3.01, 4.95, 3.73, 1.37, 0.78	2.97, 4.76, 3.57, 1.35, 0.77
ΔG, ΔQ	0.22, 0.79	0.22 ± 0.02, 0.80 ± 0.1[a]
$\mathbf{W}$, km/s	(−14.76, −2.52, −6.79)	(−14.75, −2.68, −6.62)
V_s, km/s	321.2	322.0
Δt, min	28.45	28.4

[a]The uncertainties of ΔG and ΔQ shown in the best fit result come from the uncertainties of the plasma betas.

Table 7. The "True Answer" and the Best Fit Values of the Synthetic Perpendicular Shock ($\theta_{BN} = 90°$)

Parameter	"True Answer" Value	Best Fit Value
$\mathbf{B}_1$, nT	(0.00, −10.00, 0.00),	(−0.05, −9.84, −0.09),
$\mathbf{B}_2$, nT	(0.00, −15.00, 0.00)	(0.03, −15.16, −0.14)
N_{eq1}, N_{eq2}, cm^{-3}	8.00, 12.00	8.2, 12.6
ξ_1, ξ_2	1.00, 1.00	0.98, 1.02
β_1, β_2	1.00, 1.07	1.01, 1.07
y	0.667	0.649
m	1.500	1.541
θ_{BN}, deg	90.0	88.9
V_A, km/s	77.1	75.1
$\hat{n}$	(−1.0000, 0.0000, 0.0000)	(−0.9998, −0.0144, 0.0120)
u	1.500	1.541
z (=yu)	1.000	∼1.000
M_A, M_{AN}, M_{AN2}, M_F, M_{F2}	2.00, −, −, 1.47, 0.79	1.92, 98.77, 79.56, 1.41, 0.73
ΔG, ΔQ	0, 0	-0.04 ± 0.06, -0.14 ± 0.17[a]
W, km/s	(−51.41, 0.00, 0.00)	(−50.74, −0.27, 0.61)
V_s, km/s	584.2	574.4
Δt, min	18.20	18.24

[a]The uncertainties of ΔG and ΔQ shown in the best fit result come from the uncertainties of the plasma betas.

[47] Here, the data means of the upstream and downstream magnetic fields are set to be (1.95, 1.50,0.28) and (−2.40, 3.10, 1.00) nT, the data means of upstream and downstream number density (N_{eq}) are 18 and 34 cm^{-3}, and the data means of upstream and downstream anisotropy parameters are 0.98 and 1.02, respectively. The data SD of the magnetic field is 0.15 nT, the SD of the number density is 1.5 cm^{-3}, the SD of the anisotropy parameter is 0.04, the SD of the plasma beta is 0.4, the SD of each component of **W** is 2.2 km/s, and the SD of Δt is 0.1 min.

[48] We have tried Method A to check this shock, and the fit is not good. Now we use Method B to analyze this shock. The best fit parameters of this shock are listed in Table 6. It can be seen that the best fit solution is very close to the "true answer." The estimated shock normal is only ∼0.6° off from the "true answer" shock normal. The estimated ΔG and ΔQ also agree with the "true answer." Thus the Method B works for the shock where ΔG and ΔQ are needed.

3.3. Perpendicular and Parallel Shocks

[49] We apply our procedure to an exactly perpendicular shock, which requires neither ΔG nor ΔQ. For the exactly perpendicular shock, $z = 1$, which makes M_{AN} to be infinite, and there is no defined HT frame of reference. Thus to construct the "true answer" shock structure, we have to derive new relations between the shock parameters. The new relations are derived under the shock frame of reference of a perpendicular shock. The details of deriving the shock parameters are provided in Appendix C. Table 7 shows these parameters of the "true answer."

[50] Likewise, we apply a 1/2-SD shift to the magnetic field and plasma data so that the data means of the magnetic fields are $\mathbf{B}_1$ = (0.13, −9.88, −0.12) and $\mathbf{B}_2$ = (0.12, −14.87, 0.12) nT, which are off from the exactly perpendicular shock solutions shown in Table 7. The shifted magnetic field data means make the derived shock normal, $\hat{n}$ = (−0.722, 0.069, 0.688), at an angle as large as ∼43° off from the "true answer" shock normal. Now we apply Method B. The best fit solution is also shown in Table 7. As can be seen, the fit is still good for this shock. The best fit shock normal is ∼1.1° off from the "true answer" shock normal. We also try Method A to analyze this shock, and the result is close to that estimated from Method B.

[51] The same analyses are also made for two other synthetic shocks with θ_{BN} = 89° and 1°, respectively. Figure 4 shows a comparison of the best fit and the "true answer" parameters for the synthetic shocks, discussed here, with different shock normal angles. We repeat the same procedure for five times and calculate the mean and SD for the five best fit solutions. The x axis indicates the "true answer" shock normal angle. Figures 4a–4c show the difference between the best fit and the "true answer" θ_{BN}, M_A, and M_F, respectively. The error bars for these plots represent the SDs calculated from the five contiguous estimations. Figure 4d shows the angle, α, between the best fit and the "true answer" shock normal vectors. The error bars also represent the SDs calculated from the five contiguous estimations. As can be seen, the solutions are stable and reliable. The SDs in Figure 4 can be considered as confidence intervals for the solutions of shock parameters.

4. Application to Real Shocks

[52] In this section, two real shocks observed in interplanetary space by both the WIND and Geotail spacecraft are analyzed by our method. One of these shocks, which is associated with a magnetic cloud, has been investigated by *Lepping et al.* [1997], while both of these two shocks have been investigated by *Berdichevsky et al.* [2000]. Using the WIND data of the magnetic field and plasma and the given information about the arrival times and the positions of WIND and Geotail, we apply our procedure to these two cases. They are discussed below.

4.1. The 19 October 1995 Shock

[53] This shock has been already analyzed and reported by *Lepping et al.* [1997] and is considered as a shock-like structure. They did not confirm whether it is a fast-mode shock, since the estimated downstream fast Mach number is larger than 1. However, the investigation of *Berdichevsky et al.* [2000] reported that it is a fast shock with an upstream Mach number of 1.3. Here, we re-analyze the shock with our method.

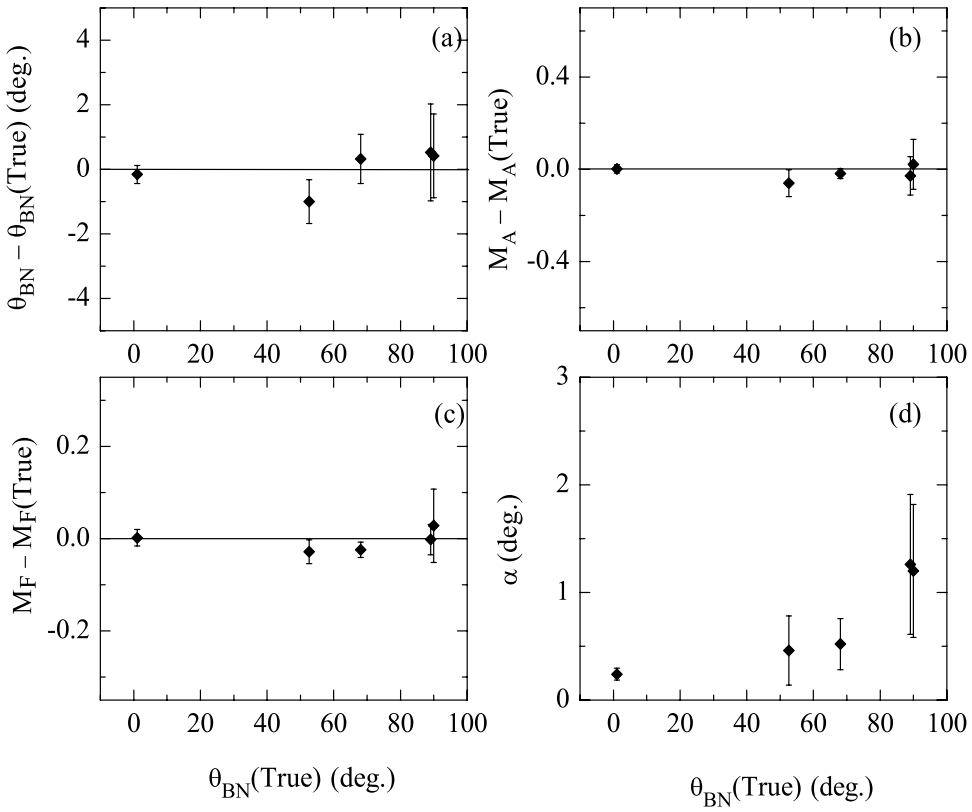

Figure 4. Comparison of the best fit and the "true answer" parameters: The *x* axis indicates the "true answer" shock normal angle. Figures 4a–4c show the differences between the best fit and the "true answer" θ_{BN}, M_A, and M_F. The error bars for these plots represent the SDs calculated from five contiguous estimations. Figure 4d shows the angle, α, between the best fit and the "true answer" shock normal vectors. The error bars also represent the SDs calculated from the five contiguous estimations.

[54] In our analysis, the observed parameters are obtained from the WIND spacecraft. The magnetic field data come from the magnetic field investigation (MFI) magnetometer, which has a 3-s time resolution. The ion data (protons and alpha particles) of number density, temperature, and bulk velocity come from the solar wind experiment (SWE) plasma instrument, which has an 80-s time resolution. The electron temperature and anisotropy ($A_e \equiv T_{e\|}/T_{e\perp}$) data also come from the SWE. $T_{e\|}$ and $T_{e\perp}$ are parallel and perpendicular electron temperatures defined in magnetic field-aligned coordinates. The proton anisotropy, $A_p \equiv T_{p\|}/T_{p\perp}$, comes from the three-dimensional plasma analyzer (3DP), where $T_{p\|}$ and $T_{p\perp}$ are parallel and perpendicular proton temperatures defined in magnetic field-aligned coordinates as well. This data set has a 3-s time resolution. All the raw data are extracted from the Web site of Coordinated Data Analysis Web (CDAWeb) published by the Goddard Space Flight Center and the M.I.T. Space Plasma Group. The GSE coordinate system is used in this study.

[55] In calculating the plasma parameters (ρ, β, **V**, and ξ), we include the contribution of alpha particles and/or electrons. The plasma density is calculated from

$$\rho = m_p n_p + m_a n_a = m_p(n_p + 4n_a), \tag{23}$$

where m_p and m_a are the masses of proton and alpha particle, and n_p and n_a are the number densities of protons and alpha particles, respectively. The plasma beta can be calculated from

$$\beta = \frac{P_e + P_p + P_a}{B^2/2\mu_0} \approx \frac{(n_p + \mathbf{2}n_a)kT_e + n_p kT_p + n_a kT_a}{B^2/2\mu_0}, \tag{24}$$

where T_e, T_p, and T_a are the temperatures of the electrons, protons, and alpha particles. Moreover, the center of mass velocity, **V**, is calculated from

$$\mathbf{V} = \frac{m_p n_p \mathbf{V}_p + m_a n_a \mathbf{V}_a}{m_p n_p + m_a n_a} = \frac{n_p \mathbf{V}_p + 4n_a \mathbf{V}_a}{n_p + 4n_a}, \tag{25}$$

where $\mathbf{V}_p$ and $\mathbf{V}_a$ are the bulk velocities of protons and alpha particles, respectively.

[56] To calculate the plasma anisotropy parameter ξ, we have the data for proton and electron anisotropies. In general the electrons behave more or less isotropic. However, usually the electron thermal pressure dominates the plasma thermal pressure in interplanetary shock; thus the contribution of electron anisotropy to the value of ξ should also be considered. The ξ can be expressed as

$$\begin{aligned}\xi &= 1 - \left(\frac{p_{p\|} - p_{p\perp}}{B^2/\mu_0} + \frac{p_{a\|} - p_{a\perp}}{B^2/\mu_0} + \frac{p_{e\|} - p_{e\perp}}{B^2/\mu_0}\right) \\ &= 1 - \left(\frac{3}{2}\frac{(A_p - 1)\beta_p}{A_p + 2} + \frac{3}{2}\frac{(A_a - 1)\beta_a}{A_a + 2} + \frac{3}{2}\frac{(A_e - 1)\beta_e}{A_e + 2}\right),\end{aligned} \tag{26}$$

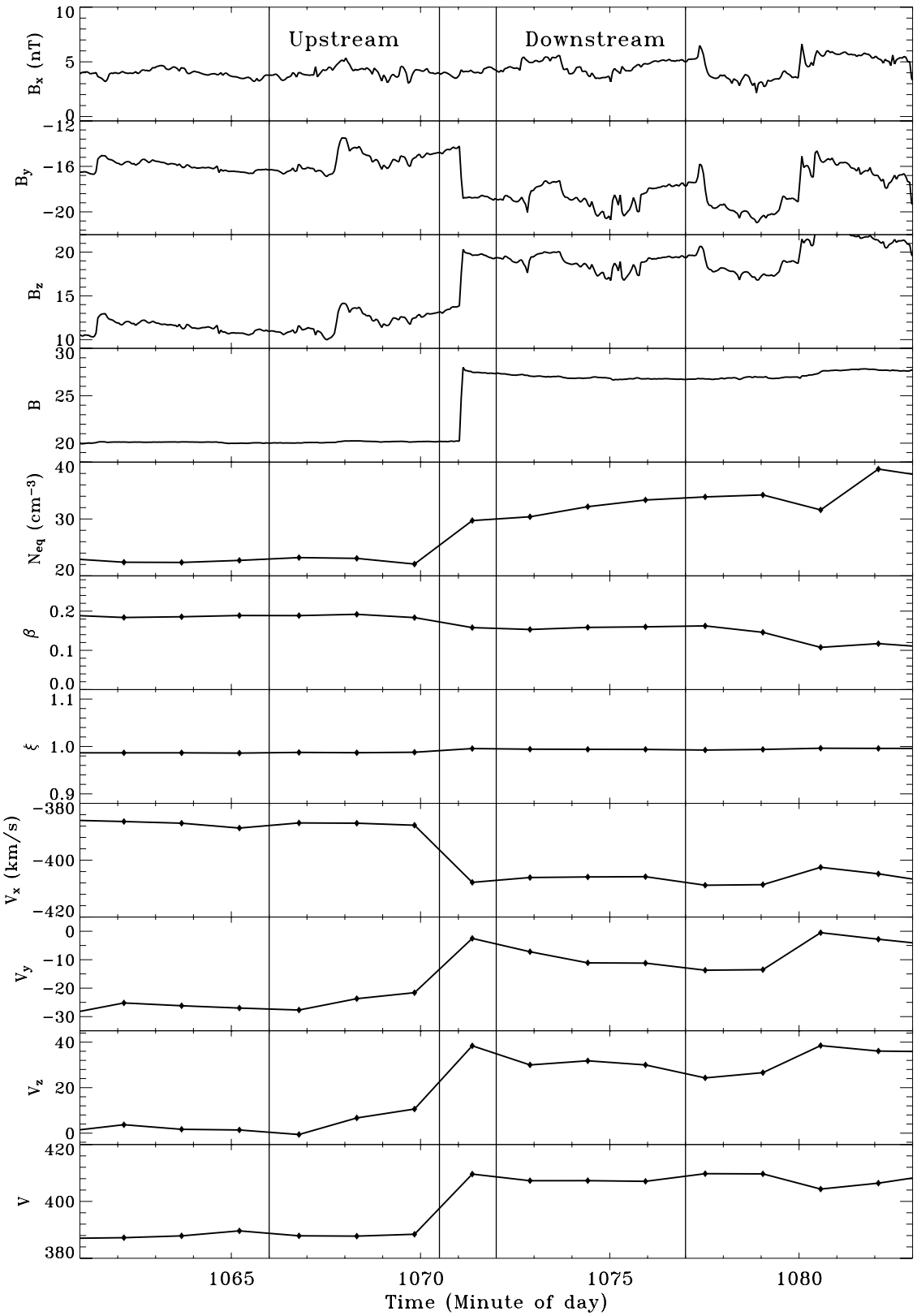

Figure 5. The data for the magnetic field, plasma density, plasma beta, anisotropy parameter, and velocity of the shock on 19 October 1995: Here, the coordinate system is in GSE. The time unit used is in minutes counted from the beginning of a day. $N_{eq} = \rho/m_p$, is the plasma number density, where m_p is the proton mass. The vertical lines indicate the data interval for the upstream and downstream observables. The shock layer is at ~1071 min of the day.

Table 8. Data Means and SDs of the 19 October 1995 Shock

Observable	Mean	Standard Deviation
$\mathbf{B}_1$, [a] nT	(4.05, −15.57, 11.99),	(0.46, 0.84, 1.09),
$\mathbf{B}_2$	(4.58, −18.67, 18.81)	(0.58, 0.93, 0.87)
N_{eq1}, N_{eq2}, cm^{-3}	22.79, 31.96	0.62, 1.49
ξ_1, ξ_2	0.987, 0.994	0.001, 0.001
β_1, β_2	0.188, 0.157	0.005, 0.004
$\mathbf{W}$, km/s	(−18.5, 14.5, 25.4)	(0.5, 4.5, 5.9)
Δt, min	31.97	0.25

[a]The coordinate system is GSE.

where $p_{p\|}$ ($p_{p\perp}$), $p_{a\|}$ ($p_{a\perp}$), and $p_{e\|}$ ($p_{e\perp}$) are parallel (perpendicular) thermal pressures of protons, alpha particles, and electrons, and A_p, A_a, and A_e are the anisotropies, while β_p ($\equiv P_p/(B^2/(2\mu_0))$), β_a, and β_e are the plasma betas of protons, alpha particles, and electrons. Here, the thermal pressure P_α for each ion species can be expressed as

$$P_\alpha = \frac{p_{\alpha\|} + 2p_{\alpha\perp}}{3}, \tag{27}$$

where α represents the specific ion species. Let us now assume that the alpha particles have nearly the same amount of anisotropy as the protons. That is, $A_a \sim A_p$. The above expression can further be approximated as

$$\xi \approx 1 - \frac{3}{2}\frac{(A_p - 1)}{A_p + 2}(\beta_p + \beta_a) - \frac{3}{2}\frac{(A_e - 1)}{A_e + 2}\beta_e. \tag{28}$$

[57] The data of the magnetic field and plasma are shown in Figure 5. The time unit used here is in minutes counted from the beginning of a day. The vertical lines indicate the data that is used for the upstream and downstream observables. In order to have at least three observation points for the plasma observables, we use about 5 min intervals for the upstream and downstream regions, respectively.

[58] This shock was observed at 1751:03 UT by WIND located at (176.09, −2.21, −12.75) R_E (GSE). It was also observed by Geotail at 1823:01 UT at the location (13.71, −1.17, 1.06) R_E. Thus the spatial displacement between the two spacecraft is $\Delta\mathbf{R}$ = (−162.4, 1.1, 13.8) R_E, and the difference between the shock arrival times is $\langle\Delta t\rangle$ = 31.97 min, with an error of ∼0.25 min. The associated means and SDs for all the observables are shown in Table 8.

[59] Table 9 shows the parameters directly calculated from the means of the observed magnetic fields, plasma densities, anisotropy parameters, and plasma betas. The resultant fast Mach numbers are M_F = 2.30 and M_{F2} = 1.45, which is not permissible for a fast shock. Furthermore, the observed mean center of mass velocities in the upstream and downstream regions are $\mathbf{V}_1$ = (−387.2, −24.7, 5.3) km/s and $\mathbf{V}_2$ = (−405.6, −10.1, 30.8) km/s, respectively. Thus the velocity difference $\langle\mathbf{W}\rangle$ = (−18.5, 14.5, 25.5) km/s, which is quite different from the velocity difference directly calculated from the means of the magnetic fields and the plasma moments via equation (8).

[60] We apply Method B to this shock. Note that to calculate the loss function, we let the systematic error in equation (15) be $\sigma_k'' = (1/2)\sigma_k'$ for each variable. Then, a best fit solution is obtained by finding a minimum value of the loss function, $L_{\min}$. Here $L_{\min}$ = 1.8. The corresponding values of the best fit solution are shown in Table 10. It is found that the estimated magnetic fields and plasma moments deviate from the means of the corresponding observables by no more than one sigma. The upstream fast Mach number is larger than 1, and the downstream fast Mach number is less than 1. Meanwhile, the upstream and downstream normal Alfvén Mach numbers are both larger than 1. Therefore this is a fast magnetosonic shock. As can also be seen in Table 10, the ΔG and ΔQ are quite small. It appears that for this shock the ΔG and ΔQ are unneeded. We have also tried Method A. The result is close to that one estimated by Method B.

[61] We compare our results with that of the other methods. As can be seen in Table 10, the shock normal vector estimated by *Lepping et al.* [1997] is (−0.558, 0.714, 0.422) (ϕ = 128° and θ = 25°), while the shock normal vector estimated by our method is (−0.549, 0.703, 0.451) (ϕ = 128.0° and θ =26.8°). There is an angular difference of ∼1.9° between the two estimated vectors. The shock speed in the spacecraft frame of reference estimated by our method is 320 km/s, which is different from that estimated by *Lepping et al.* [1997] at 338 km/s. The shock speed in the upstream solar wind frame of reference estimated by *Lepping et al.* [1997] is 137.4 km/s. Using this value and values of the upstream magnetic field intensity (B ∼ 20 nT) and plasma number density ($N \sim 20$ cm^{-3}) (see the "C" discontinuity in Figure 1 of *Lepping et al.* [1997]), we can estimate the Alfvén Mach number (V_{n1}/V_A), $M_A \sim 1.4$. On the other hand, the Alfvén Mach number estimated by our method is M_A = 1.37. These two values are close.

[62] *Berdichevsky et al.* [2000] used the preaveraged method [e.g., *Abraham-Shrauner*, 1972; *Abraham-Shrauner and Yun*, 1976] and the least squares fitting method to the RH relations of *Viñas and Scudder* [1986] and *Szabo* [1994] to find the shock normal and the shock parameters. They obtained an optimal shock normal, for which the results of the first and second methods coincide within an acceptable range. The shock normal vector estimated by *Berdichevsky et al.* [2000] for this shock is (−0.575, 0.736, 0.358) (ϕ = 128° and θ = 21°). Thus the shock normal

Table 9. Values of the Derived Parameters Calculated From the Means of the Observed Magnetic Fields, Plasma Densities, Anisotropy Parameters, and Plasma Betas of a Real Shock on 19 October 1995

Parameter	Values
y	0.713
m	1.340
θ_{BN}, deg	61.3
V_A, km/s	91.7
$\hat{n}$	(−0.291, 0.862, 0.414)
M_A, M_{AN}, M_{AN2}, M_F, M_{F2}	2.44, 5.07, 4.28, 2.30, 1.45
ΔG, ΔQ	0.21, 0.37
$\mathbf{W}$, km/s	(−18.2, 52.5, 32.8)

Table 10. Best Fit Solution of the 19 October 1995 Shock

Parameter	Value	L[a]	B[b]
$\mathbf{B}_1$, nT	(4.20, −14.96, 11.76),		
$\mathbf{B}_2$	(4.23, −19.11, 18.28)		
N_{eq1}, N_{eq2}, cm^{-3}	22.8, 31.6		
ξ_1, ξ_2	0.987, 0.994		
β_1, β_2	0.188, 0.157		
y	0.723		
m	1.374		1.35 ± 0.02
θ_{BN}, deg	67.3	perpendicular	80–90
V_A, km/s	88.9	97.5[c]	
$\hat{n}$	(−0.549, 0.703, 0.451)	(−0.558, 0.714, 0.422)	(−0.575, 0.736, 0.358)
ϕ, θ, deg	128.0, 26.8	128, 25	128, 21
u	1.430		
z (=yu)	1.034		
M_A, M_{AN}, M_{AN2},	1.37, 3.56, 3.03,	1.4[d], −, −,	1.4, −, −,
M_F, M_{F2}	1.29, 0.80	2.7, 1.96	1.3, −
ΔG, ΔQ	0.01 ± 0.02, 0.03 ± 0.04		
$\mathbf{W}$, km/s	(−18.5, 18.4, 23.7)		
V_s, km/s	320	338	
Δt, min	32.0	32.4	

[a]Results of *Lepping et al.* [1997].
[b]Results of *Berdichevsky et al.* [2000].
[c]We estimate it from the upstream magnetic filed intensity and plasma density shown in Figure 1 of *Lepping et al.* [1997].
[d]Dividing the shock speed (137.4 km/s) in the upstream solar wind frame estimated by *Lepping* [1997] by the upstream Alfven speed V_A.

vectors estimated by our method and by *Berdichevsky et al.* [2000] have an angular difference of ∼5.9°. The shock speed in the upstream solar wind frame estimated by *Berdichevsky et al.* [2000] is 137 km/s, and the Alfvén Mach number is 1.4. On the other hand, the fast magnetosonic Mach number estimated by *Berdichevsky et al.* [2000] is 1.3, while that by our method is 1.29. The Mach numbers estimated by our method and by *Berdichevsky et al.* [2000] are close.

4.2. The 23 March 1995 Shock

[63] This shock was observed at 0937:24 UT by WIND located at (213.75, 39.67, 17.50) R_E and was also observed by Geotail at 1040:00 UT, at (−5.03, 28.87, −3.85) R_E. The displacement between the two spacecraft is $\Delta\mathbf{R}$ = (−218.8, −10.8, −21.4) R_E, and the averaged time delay is $\langle\Delta t\rangle$ = 62.6 min. The observed data means are listed in the second column of Table 11. The lower part of this column shows the corresponding parameters directly calculated from the data means of the observed magnetic fields, plasma densities, anisotropy parameters, and plasma betas.

[64] The result of Method A (not shown here) indicates that the fit is not good. Unless the data were given very large errors, the model without ΔG and ΔQ cannot be applied to this shock. Now we use Method B to analyze this case. The best fit values of the upstream and downstream parameters are listed in Table 11. It is found that in this case, $\Delta G = 0.08 \pm 0.04$ and $\Delta Q = 0.49 \pm 0.15$. Note that the uncertainties of ΔG and ΔQ come from the uncertainties of the plasma betas. The result, using the present data set, indicates that the shock needs significant amounts of ΔG and ΔQ in order to satisfy the whole set of RH relations.

Table 11. Parameters From the Data Means and From Our Method for the Real IP Shock on 23 March 1995

Parameter	Data Mean[a]	Best Fit	B[b]
$\mathbf{B}_1$, nT	(0.10, 2.45, −3.47),	(0.16, 2.68, −3.66)	
$\mathbf{B}_2$	(1.50, 4.75, −6.25)	(1.07, 4.69, −6.40)	
N_{eq1}, N_{eq2}, cm^{-3}	10.30, 16.98	9.77, 17.34	
ξ_1, ξ_2	0.92, 1.14	0.88, 1.15	
β_1, β_2	3.09, 1.65	3.09, 1.65	
$\mathbf{W}$, km/s	(−38.1, 2.6, −3.1)	(−34.3, 3.4, −4.6)	
Δt, min	62.6	62.2	
y	0.606	0.563	
m	1.881	1.762	2.2
θ_{BN}, deg	69.6	77.1	69 ± 6
V_A, km/s	28.9	31.7	
$\hat{n}$	(−0.908, 0.052, −0.416)	(−0.966, 0.153, −0.209)	(−0.951, 0.168, −0.259)
ϕ, θ, deg	176.7, −24.6	171.0, −12.1	170, −15
u	1.973	1.793	
z (=yu)	1.196	1.010	
M_A, M_{AN}, M_{AN2}, M_F, M_{F2}	0.91, 2.61, 2.03, 0.49, 0.25	2.49, 11.12, 8.34, 1.32, 0.69	3.6, −, −, 1.8, −
ΔG, ΔQ	−2.98, −3.18	0.08 ± 0.04, 0.49 ± 0.15	
V_s, km/s	296.8	365.7	

[a]The SD of $\mathbf{B}_1$ is (0.10, 0.24, 0.34) nT, the SD of $\mathbf{B}_2$ is (0.29, 0.22, 0.29) nT, the SD of N_{eq1} and N_{eq2} are 0.32 and 0.41 cm^{-3}, the SD of ξ_1 and ξ_2 are 0.05, 0.03, the SD of β_1 and β_2 are 0.37 and 0.16, the SD of $\mathbf{W}$ is (3.5, 3.1, 2.9) km/s, and the SD of Δt is 1.0 min.
[b]Results of *Berdichevsky et al.* [2000].

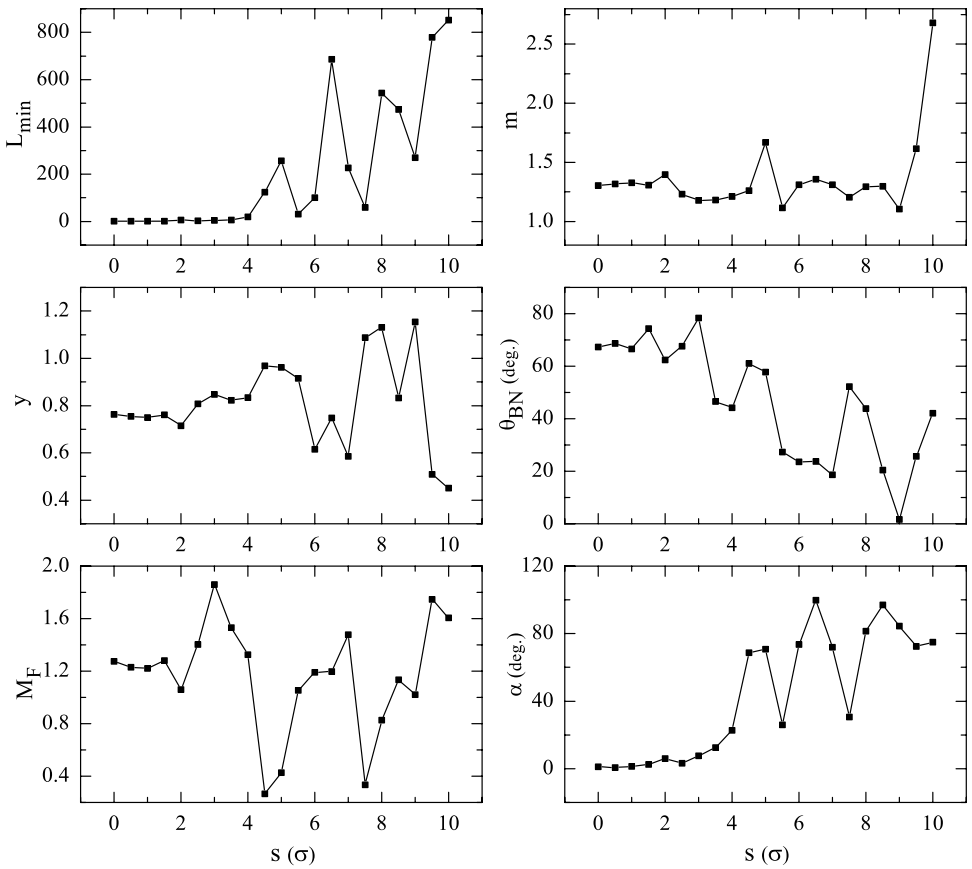

Figure 6. The value of the minimum loss function and the values of the estimated parameters with various shifts, *s*, which are applied to the first simulation case: The *s* is normalized by the SD. The α represents the angle between the estimated and the "true answer" shock normal.

[65] As can be seen in Table 11, the shock normal estimated by our method is (−0.966, 0.153, −0.209) (ϕ = 171° and θ = −12.1°). The shock normal vector estimated by *Berdichevsky et al.* [2000] is (−0.951, 0.168, −0.259) (ϕ = 170° and θ = −15°). These two shock normal vectors have an angular difference of ∼3.1°. The Alfvén Mach number estimated by our method is 2.49, and that by *Berdichevsky et al.* [2000] is 3.6. On the other hand, the fast Mach number estimated by our method is 1.32, and that by *Berdichevsky et al.* [2000] is 1.8. The Mach numbers estimated by our method and by *Berdichevsky et al.* [2000] are different.

[66] The difference in Mach numbers between our results and the results of *Berdichevsky et al.* [2000] may be caused by several reasons. One of the reasons is the difference in the selected upstream and downstream intervals. The upstream and downstream regions used by our method are selected to be (0933:00–0937:00 UT) and (0937:50–0941:00 UT), respectively. The interval lengths are less than 5 min, and the intervals are near the shock layer. In the study of *Berdichevsky et al.* [2000], they choose an interval length of ∼6–20 min. The upstream and downstream regions used for the preaveraged method are selected to be (0912–0921 UT) and (0945–0952 UT), respectively [see *Berdichevsky et al.*, 2000, Table A.1].

[67] Another possible cause is that the shock plane may not be flat and/or that the medium within which the shock propagates may be nonuniform. Our method, using two spacecraft arrival time, can obtain a good result only when a shock plane is flat and when the shock propagates at a constant shock speed between the two spacecraft. If the shock were not in such a condition, our fitting method would have some errors in shock speed.

5. Error Analysis in Our Synthetic Simulations

[68] In this section we estimate the reliability of the procedure. First, we give different amount of shifts of the means for the first synthetic simulation case. For analyzing this shock in section 3.1, the data means for the magnetic field, plasma density, and anisotropy parameter are assumed to have a random shift from the "true answer," and the magnitude of the shift is ∼1/2 of the sample SD. Now we define a shift parameter, *s*, $s \equiv (data\ mean - true)/\sigma'$, where σ' is the SD. The *s* is the discrepancy of the data mean from the "true answer" for the magnetic field, plasma density, and anisotropy parameter normalized by their SDs. It represents the size of systematic error occurring in the simulated data. We look for the variations of the best fit solution and the loss function when a different *s* is applied. The result is shown in Figure 6. To calculate the loss function for the synthetic shocks and the two real shocks in sections 3 and 4, the systematic error in equation (15) is assumed to be $\sigma'' = (1/2)\sigma'$. The ratio is fixed in this

estimation. The $L_{\min}$ shown in Figure 6 is the minimum loss function value for each case, and α is the angle between the best fit and the "true answer" shock normal.

[69] As can be seen in Figure 6, the loss function increases with s, while the solution deviates more from the "true answer." Furthermore, the angle α increases with s as well. The results show that the solution estimated by our method is reliable as long as the difference between the observed means and the "true answer" is not larger than 2 sigmas in errors.

[70] In our simulation study in section 3, the data means of the velocity difference **W** did not shift from the "true answer" because we consider that systematic errors in the velocity measurements are likely to be subtracted out in **W** if the systematic errors are symmetric on the two sides of a shock. In addition, the velocity measurements are the most reliable parameters in solar wind plasma measurements. Now, in addition to the systematic errors in the magnetic field and plasma density, we also apply a small ($\sim$1/2 SD) and asymmetric systematic errors to the upstream and downstream velocities. An example is presented here. We reanalyze the first synthetic shock. The data of the upstream and downstream velocities are randomly shifted such that the data means are $\langle \mathbf{V}_1 \rangle$ = (−429.5, 9.4, −30.1) and $\langle \mathbf{V}_2 \rangle$ = (−450.2, 12.3, −17.4) km/s, respectively. The corresponding mean of **W** is $\langle \mathbf{W} \rangle$ = (−20.6, 2.9, 12.7) km/s. Here, all the other data means and SDs are the same as in Table 3. The result shows that the best fit shock normal is (−0.955, 0.055, 0.291), which is $\sim$1.3° off from the "true answer." The best fit shock normal angle is θ_{BN} = 69.0°, and upstream Alfvén and fast Mach number are M_A = 1.32 and M_F = 1.20. So, the result is still good.

[71] As in the error analysis shown in Figure 6 for the systematic errors in magnetic field, plasma density, and anisotropy parameter, an analysis have been made using different amount of data shift for the velocities. Here, the data means for the magnetic field and plasma density are set to have a shift of only $\sim$1/2 SD from the "true answer" value. The result also shows for much larger systematic errors, the result becomes unreliable.

[72] When the Method B is used, we have two degrees of freedom due to giving two more parameters ΔG and ΔQ. As mentioned in section 3.1, the uncertainties of the ΔG and ΔQ as well as the fast Mach numbers are mainly determined from the uncertainties of the plasma betas. The two degrees of freedom can compromise with all the errors occurring in β_1 and β_2. Thus the other parameters, such as the shock normal, which can be fitted well by virtue of equations for velocity and for arrival time, and the loss function, will not be adjusted by the errors of β_1 and β_2.

[73] When the Method A is used, the situation is quite different. The β_1, β_2, and the other parameters are required to satisfy equations (9) and (10) as well as all the other conservation equations with ΔG = 0 and ΔQ = 0. For a better fitting of β_1 and β_2, the procedure will force all the parameters to compromise with the errors of β_1 and β_2. Under this condition, other parameters and hence the shock normal are adjusted.

[74] In Method A the plasma betas can be fitted. Here we reanalyze the first synthetic shock by introducing systematic errors occurring in both the velocities and plasma betas. Here the data means of the velocities are assumed to be $\langle \mathbf{V}_1 \rangle$ = (−429.5, 9.4, −30.1) and $\langle \mathbf{V}_2 \rangle$ = (−450.2, 12.3, −17.4) km/s. Thus the mean of **W** is $\langle \mathbf{W} \rangle$ = (−20.6, 2.9, 12.7) km/s. The data of plasma betas are randomly shifted by $\sim$1/2 SD from the "true answer," so their means are now $\langle \beta_1 \rangle$ = 0.260 and $\langle \beta_2 \rangle$ = 0.251. The data means for the other observables are the same as in Table 3. Following our procedure, we obtain that the best fit θ_{BN} = 70.1°, M_A = 1.35, M_F = 1.26, and the best fit shock normal vector is (−0.949, 0.062, 0.301). The best fit shock normal vector has an angular difference of $\sim$1.7° from the "true answer" shock normal. The best fit β_1 and β_2 are 0.265 and 0.253, which are close to the "true answer."

[75] In order to determine the uncertainties propagating from the plasma betas to ΔG and ΔQ as well as the fast Mach numbers, we show how the ΔG, ΔQ, and the fast Mach numbers change as the plasma betas change for the first and second simulation study cases. Figure 7 shows the values of the ΔG and ΔQ at various plasma betas. Figure 7a and Figure 7b are for the first case, and Figure 7c and Figure 7d are for the second case. The plasma beta values are normalized by their SDs, $\sigma'_{\beta 1}$ and $\sigma'_{\beta 2}$. Here, β_{1T} and β_{2T} represent the values of "true answer" for the upstream and downstream plasma betas, respectively. In Figure 7, the values of the "true answer" for y, m, θ_{BN}, ξ_1, and ξ_2 are used. It can be seen that if the β_1 and/or β_2 shifts are no more than 1 sigma, the values of ΔG and ΔQ are not strongly affected. In general the observed plasma betas should deviate from the "true answer" no more than 1 sigma. The means of β_1 and β_2 are within the circles indicated in Figure 7. Thus the best fit values will be also within the circles. Therefore the radii of circles can represent the uncertainties propagating from the plasma betas to ΔG and ΔQ. Figures 8a through 8d show the values of the fast Mach numbers at various plasma betas for the first and second simulation cases, respectively. It can also be seen that the fast Mach numbers are not strongly affected within 1 sigma of the errors of the plasma betas. The square in Figure 8a indicates the range within which the solution of fast Mach number can be. The results shown in Figure 7 demonstrate that if a shock actually has a significant amount of ΔG and/or ΔQ, our method can really find them, with an uncertainty depending on the errors of the observed plasma betas.

6. Discussion and Conclusion

[76] In this study we present a shock fitting procedure, which is separated under two conditions. In one procedure, Method A, we use the whole set of classical RH relations. Another procedure, Method B, utilizes the modified RH relations, which include parameters ΔG for the equivalent "normal momentum flux" and ΔQ for the equivalent "heat flow," which are possibly due to waves/turbulences, energetic particles, and/or other causes.

[77] Our procedure uses the two spacecraft observations. However, it works even if only one spacecraft observation is available. Then, equation (15) will not be used and the Δt term is excluded from the loss function. Thus we have 15 variables. Now we recalculate the first synthetic shock case under this condition. The results are m = 1.322, y = 0.751, θ_{BN} = 68.6°, M_A = 1.32, M_F = 1.21, and the estimated shock normal is $\hat{n}$ = (−0.955, 0.074, 0.287), which is $\sim$1.0°

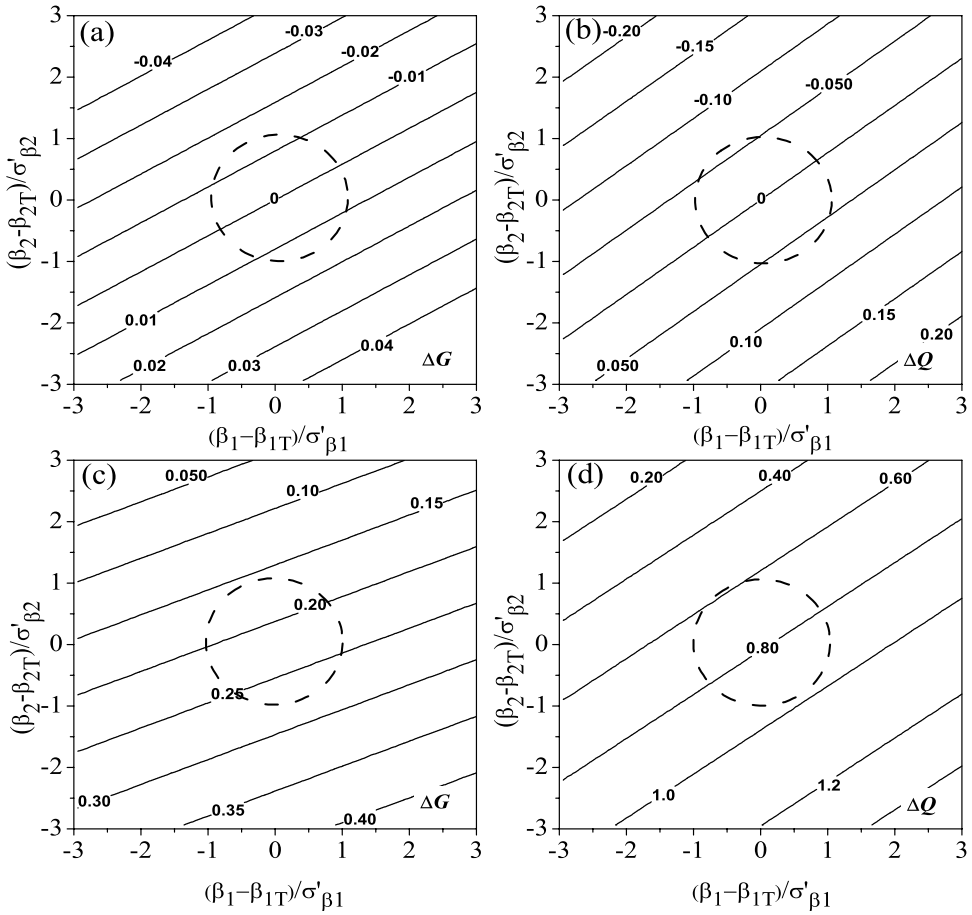

Figure 7. The ΔG and ΔQ as functions of the plasma betas for the simulated cases: (a)–(b) the first case and (c)–(d) the second case. The plasma betas are normalized by their SDs, and β_{1T} and β_{2T} represent the values in "true answer" for the upstream and downstream plasma betas, respectively. The dashed circles indicate 1 sigma error for the betas. The values of the "true answer" for y, m, θ_{BN}, ξ_1, and ξ_2 are used in this figure.

off from the "true answer" shock normal. In addition, the estimated shock speed is 502.8 km/s. The $\Delta G = -0.005 \pm 0.008$ and $\Delta Q = -0.02 \pm 0.03$. The result is still close to the "true answer."

[78] Our procedure can also be applied to a subset of RH relations when the conservation equations for normal momentum and energy flux are not used. The "true answer" of the shock normal in the absence of the temperature data can still be found. If equations (9) and (10) for Method A (or equations (9′) and (10′) for Method B) are not used and the plasma beta is excluded from the loss function, we have only 14 variables. We recalculate the first simulation case. The results are $m = 1.321$, $y = 0.753$, $\theta_{BN} = 68.9°$, $M_A = 1.33$ and the estimated shock normal is (−0.956, 0.060, 0.288), which is ∼0.9° off from the "true answer" shock normal. The estimated shock speed is 502.8 km/s. Therefore without the information about plasma betas, our procedure still works.

[79] Our procedure is based on the RH relations that do not include the effect of alpha particle slippage pressure tensor (see definition in Appendix D). It is applicable only when the slippage of alpha particles from protons is small. With the observed bulk velocities and densities for protons and alpha particles, we investigate the slippage pressure tensor π_{ij} (see Appendix D) for the two real shocks studied here. In general the error of the thermal pressure due to data fluctuation is ∼10% of the averaged quantity. If the slippage pressure is comparable to this number, we think the error contributed by the alpha particle slippage should be taken into account in the analysis. Table 12 shows the densities and bulk velocities for the protons and the alpha particles. Here, the GSE coordinate system is used. The values of π_{ij} are listed in Table 12 as well. For comparison, we calculate the thermal energy densities of the three particle compositions in the solar wind for those two shocks. The results are also listed in Table 12. In calculating $\rho_e(v_{th,e})^2$, the electron mass is set to be (1/1800) of the proton mass. Note that for convenience the unit used for pressures (energy densities) in Table 12 is $[m_p(\mathrm{km/s})^2/\mathrm{cm}^3]$, where $m_p = 1.6726 \times 10^{-27}$ kg is the mass of a proton.

[80] As can be seen in Table 12, for both shocks, the values of π_{ij} are small in comparison with their thermal energies. Here we define R to be a ratio of the summed diagonal terms ($\pi_{xx} + \pi_{yy} + \pi_{zz}$) to the total thermal energy density on the upstream (downstream) state.

$$R = \frac{\pi_{xx} + \pi_{yy} + \pi_{zz}}{\rho_p v_{th,p}^2 + \rho_a v_{th,a}^2 + \rho_e v_{th,e}^2}. \quad (29)$$

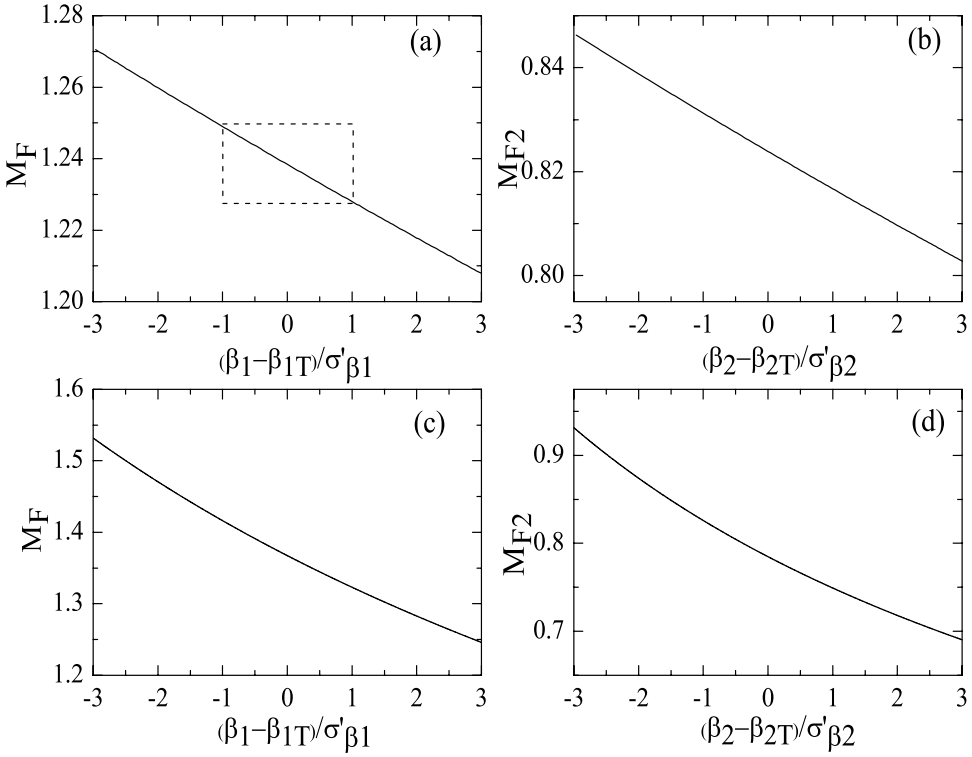

Figure 8. The fast Mach number versus the plasma beta for the simulated cases: (a)–(b) the first case and (c)–(d) the second case. The plasma betas are normalized by their SDs, and β_{1T} and β_{2T} represent the values in "true answer" for the upstream and downstream plasma betas, respectively. The values of the "true answer" for y, m, θ_{BN}, ξ_1, and ξ_2 are used in this figure.

For the 19 October 1995 shock, $R \sim 0.0004$ in the upstream region and $R \sim 0.0004$ in the downstream region. For the 23 March 1995 shock $R \sim 0.0006$ in the upstream region and $R \sim 0.001$ in the downstream region. The ratios are all much less than 1%.

[81] We try to figure out whether a small slippage pressure is a common or a particular situation for interplanetary shocks. Therefore we further investigate the slippage pressure on both sides of some interplanetary shocks observed by WIND near the ecliptic plane. We have investigated a total number of 54 interplanetary shocks observed during the period of 1995 to 2000, which include the shocks that had been analyzed by *Berdichevsky et al.* [2000]. Note that we did not select events by any special criterion. We do the analysis when the alpha particle data in the WIND-SWE data set are available. Figure 9 shows the distributions of the proton number densities and the proton speeds on both the upstream and downstream sides for those

Table 12. Slippage Pressure Tensor for the Two Real Shocks

	19 October 1995		23 March 1995	
Parameter	Upstream	Downstream	Upstream	Downstream
N_p, 1/c.c.	18.7	25.3	9.3	15.3
N_a	1	1.6	0.25	0.42
$\mathbf{V}_p$, km/s[a]	(−387.2, −24.3, 5.6)	(−405.9, −9.8, 30.6)	(−295.4, 6.0, −7.7)	(−333.5, 8.9, −11.0)
$\mathbf{V}_a$	(−387.0, −26.3, 4.1)	(−404.3, −11.3, 31.5)	(−293.4, 5.5, −3.0)	(−331.3, 6.0, −4.5)
$v_{th,p}$, km/s	14	17	19	24
$v_{th,a}$	9	13	19	24
$v_{th,e}$[b]	2090	2130	2560	2740
π_{xx}	0.2	13.1	3.7	7.3
π_{yy}	13.2	11.5	0.25	12.7
π_{zz}	7.4	4.1	20	64
π_{xy} $(=\pi_{yx})$	−1.3	−12.3	−0.9	−9.7
π_{xz} $(=\pi_{zx})$	−1	7.3	8.5	21.7
π_{yz} $(=\pi_{zy})$	10	−6.9	−2.1	−28.5
$\rho_p(v_{th,p})^2$	3665	7312	3357	8813
$\rho_a(v_{th,a})^2$	324	1082	361	968
$\rho_e(v_{th,e})^2$	50230	71830	35680	67230

[a]The GSE coordinate system is used.
[b]The unit used for π_{ij} and the thermal energy densities in this table is $[m_p(\mathrm{km/s})^2/\mathrm{cm}^3]$, where $m_p = 1.6726 \times 10^{-27}$ kg.

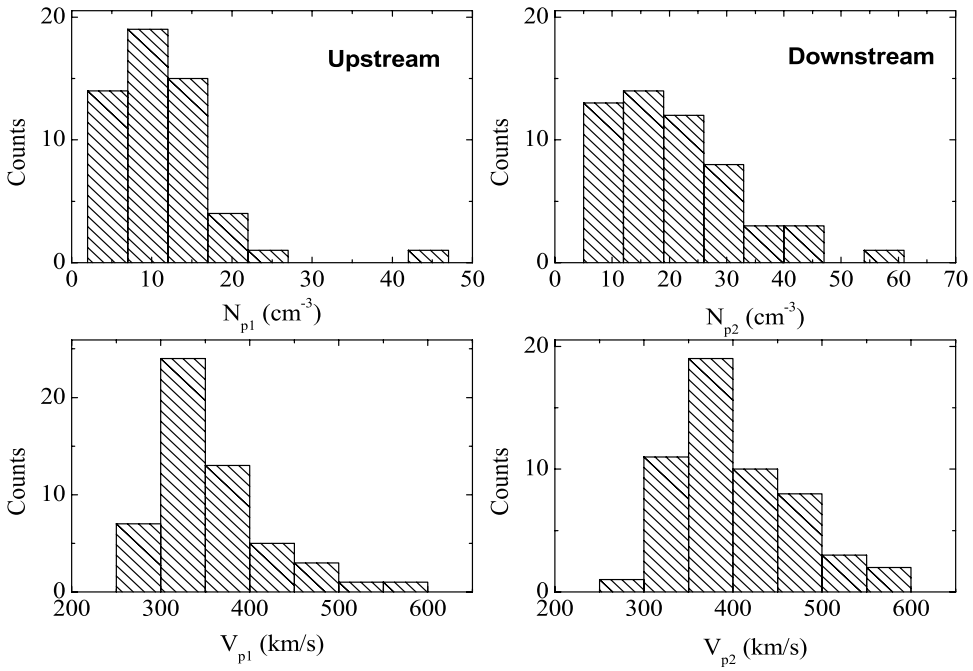

Figure 9. A statistics of the proton number density and velocity for the 54 interplanetary shocks.

54 shocks. It can be seen that the samples cover a large range of proton density (from ~2 to 45 cm^{-3} for upstream side and from ~5 to 60 cm^{-3} for downstream side). They also cover a large range of proton speed (from ~250 to 600 km/s for both sides of the shocks).

[82] Figure 10 shows the ratio, R, for the upstream and downstream sides of the total samples. It can be seen that for most cases R is less than 0.01 (1%). The maximum value of R is less than 0.035 (3.5%), which is still small comparing with the errors of the total thermal energy density. Table 13 shows the population for a specific range of R for those 54 samples. It can be seen that about 46% of the total cases have both R_1 (upstream) and R_2 (downstream) less than 0.001 (0.1%), 87% of the total cases have both R_1 and R_2 less than 0.01 (1%), and all the cases have both R_1 and R_2 less than 0.035 (3.5%). From the above results, we would like to conclude that for interplanetary shocks measured near the ecliptic plane, a small slippage pressure is a common situation and the extracted ΔG and/or ΔQ by our procedure (if they are significant) should in general be free from the effect of alpha particle slippage.

[83] Modified RH relations that involve the slippage pressure tensor will have additional terms in the conservation equations for tangential, normal momentum fluxes, and energy fluxes. By including the effect of slippage of alpha particles, the conservation equation for the tangential momentum flux across the shock layer of the modified RH relations becomes

$$\left[\rho V_n V_{T1} - \xi \frac{B_n B_{T1}}{\mu_0} + \pi_{n,T1}\right] = 0, \tag{30}$$

$$\left[\rho V_n V_{T2} - \xi \frac{B_n B_{T2}}{\mu_0} + \pi_{n,T2}\right] = 0, \tag{31}$$

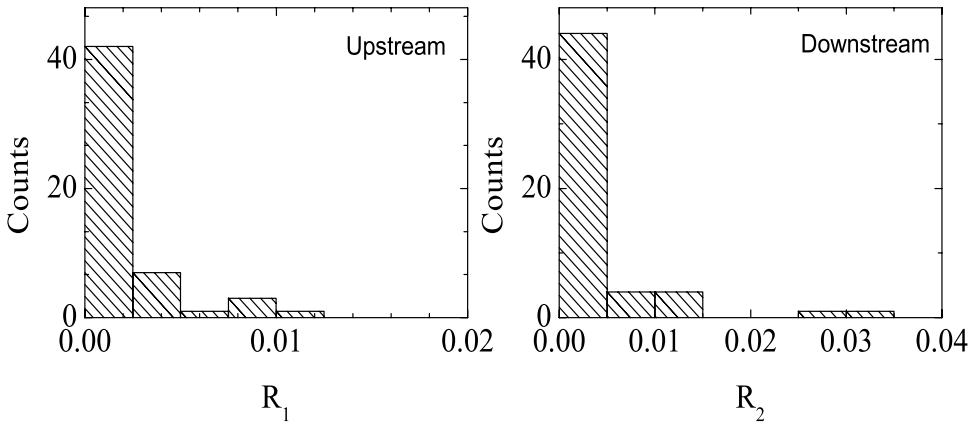

Figure 10. A statistics of the ratio of slippage pressure to thermal energy density for the 54 interplanetary shocks. R_1 is the ratio for the upstream, while R_2 is for the downstream.

Table 13. Ranges of R_1 and R_2 for the 54 Samples

R_1 and R_2	Population, %
<0.001	46%
<0.01	87%
<0.035	100%

where $\pi_{n,T1}$ and $\pi_{n,T2}$ are two elements of slippage pressure tensor. Here, n represents the shock normal direction, and $T1$ and $T2$ represent two (orthogonal) directions on the shock front. It can be shown that the magnetic coplanarity property, which has been applied very often to the shock analysis [e.g., *Lepping and Argentiero*, 1971; *Abraham-Shrauner*, 1972; *Chao et al.*, 1995; *Wu et al.*, 2000; *Berdichevsky et al.*, 2000; *Scudder*, 2005], are derived from equations (30) and (31) without slippage pressure terms [*Chao*, 1970]. However, with the additional terms in the above equations, the magnetic coplanarity property cannot be obtained. That means if the slippage pressure is not ignorable, the magnetic coplanarity theorem will not be valid. In addition, $[V_q] = 0$, one of the old RH relations (see equation (A2) in Appendix A) will not be valid as well. The magnetic coplanarity is the key criterion in our procedure. One should obtain the sequence of shock normals via the magnetic coplanarity theorem at first in order to continue the calculations. Furthermore, the fitting can be successful only when the expression for the velocity in equation (8) is valid (i.e., $[V_q] = 0$). Therefore to include the effect of alpha particle slippage in the RH relations will make our procedure very difficult to apply. A general model is a major and important development, however, is beyond the scope of the present study.

[84] Wave/turbulence and/or heat flow may be two of the sources to the momentum and energy additions in the RH relations [e.g., *Chao and Goldstein*, 1972; *Lyu and Kan*, 1986]. To extract the physical mechanism causing the ΔG and ΔQ such as the wave/turbulence and the heat flow is a complicated problem. Such a problem should be taken care of by using multifluid and/or Vlasov approaches. Some authors [e.g., *Davison and Krall*, 1977; *Yoon and Lui*, 2006] have used the Vlasov approach to construct theoretical one-fluid equations with waves. From these equations one has to derive the shock jump relations for our procedure. Even considering the simplest electrostatic wave, one can make the model very complicated. In addition, shock jump relations have to be derived based on these modified one-fluid equations in applying to our problems. For the energy addition problem, *Lyu and Kan* [1986] consider the heat flow in relations to the forward streaming and backward streaming plasma leakages. *Giacalone et al.* [1997] have tried the hybrid simulation to explain the possible excess of energy flux in the downstream side due to energetic particles accelerated at quasi-parallel shocks. Modeling the heat flow or wave/turbulence contributions to the ΔG and/or ΔQ is not the goal of the present paper.

[85] In conclusion, this study was mainly to estimate the capability of the proposed shock fitting method. Given the results, we conclude that (1) our proposed procedure is applicable only in the case of small alpha particle slippage pressure; (2) if the slippage pressure is large, we argue that the magnetic coplanarity property is not valid; (3) our proposed procedure works for both synthetic and real IP shocks, and the result is acceptable if the errors of data are not too large; (4) our procedure works for shocks with any shock normal angles, θ_{BN}; (5) in the absence of information about the plasma betas (temperatures), our procedure can still be applied to find a good shock normal vector and the associated shock parameters; and (6) for one spacecraft observation, our procedure still works.

[86] Given the assumption regarding the small slippage pressure, the magnetic coplanarity theorem in equation (2) is valid. With this theorem, one can calculate the sequence of shock normals from the magnetic field data along. The sequence of shock normals plays a key role for the calculation in our procedure. In application, the mean and error (σ') of the magnetic fields are easily evaluated from the data. In addition, the expression for $\mathbf{W}$ in equation (8) is correct only when the magnetic coplanarity property is valid. This expression makes the procedure easy to apply. The standard error of $\mathbf{W}$ that should be put into the loss function can easily be derived from the data using the approach discussed in section 3.1 (see equation (22)). Therefore the assumption regarding the small slippage pressure greatly reduces the complexity in the analysis. Moreover, with our approach, one can evaluate an accurate shock normal, shock parameters, and the possible range of the equivalent "normal momentum" and "energy" additions (ΔG and ΔQ).

[87] Our procedure is executed on a desktop PC computer. Facility of this computer includes the CPU of 3×10^9 Hz and the RAM of 3×10^9 Bytes. As the array size of $N = 10^7$ is used, the time of process of one event is $\sim$15 min. As the array size of $N = 10^8$ is used, the time is $\sim$2 hours. We believe that if an optimization in programming has been used, the time taken by the computation would be even shorter.

[88] Our procedure will be made publicly available online through the Space Environment Data Center (SEDC) Web site (http://sedc.ss.ncu.edu.tw/) of National Central University.

Appendix A: Equations Used for Fitting

[89] The RH relations are derived from the steady state anisotropic MHD conservation equations for a one-dimensional MHD shock [e.g., *Chao*, 1970; *Lyu and Kan*, 1986; *Chao et al.*, 1995]. For Method B, the RH equations are generalized to include an equivalent "normal momentum flux" term in the normal momentum flux equation and an equivalent "heat flow" term in the energy flux equation. The modified RH relations have been given by *Chao and Goldstein* [1972] and *Lyu and Kan* [1986].

$$[B_n] = 0, \tag{A1}$$

$$[V_q] = 0, \tag{A2}$$

$$[\rho V_n] = 0, \tag{A3}$$

$$[V_t B_n - V_n B_t] = 0, \tag{A4}$$

$$B_{q1} = B_{q2} = 0, \tag{A5}$$

$$\left[\rho V_n V_t - \xi \frac{B_n B_t}{\mu_0}\right] = 0, \tag{A6}$$

$$\left[\rho V_n^2 + P + \frac{1}{3}\left(\xi + \frac{1}{2}\right)\frac{B^2}{\mu_0} - \xi\frac{B_n^2}{\mu_0} + g_n\right] = 0, \tag{A7}$$

$$\left[\left(\frac{1}{2}\rho V^2 + \frac{5}{2}P + \frac{1}{3}(\xi+2)\frac{B^2}{\mu_0}\right)V_n - \xi\frac{B_n B_t}{\mu_0}V_t - \xi\frac{B_n^2}{\mu_0}V_n + q_n\right] = 0, \tag{A8}$$

where subscripts n and t represent the normal and tangential directions, and subscript q represents the direction perpendicular to the n-t plane. The square brackets denote the difference between the downstream (subscript 2) and upstream (subscript 1) states, i.e., $[Q] \equiv Q_2 - Q_1$. Here, **B** is the magnetic field, ρ, **V**, and P are mass density, center of mass velocity, and thermal pressure of the plasma, and μ_0 is the magnetic permeability in a vacuum. The g_n and q_n in equations (A7) and (A8) represent the equivalent "momentum flux" and "heat flow" in the normal direction. For Method A, these two terms are assumed zero.

[90] The RH relations discussed here do not include the pressure tensor due to alpha particle slippage relative to protons (for definition of slippage pressure tensor, see Appendix D). Here we assume that the slippage pressure tensor is unimportant. However, if the slippage is large, it can be shown that the magnetic coplanarity property is not valid and equation (A5) is incorrect. In addition, $[V_q] = 0$ in equation (A2) is incorrect as well. Thus the expression for the velocity difference (equation (8)) cannot be derived. Therefore our procedure can only be applied to cases with a small slippage pressure.

[91] The thermal pressure in equations (A7) and (A8) can be expressed as

$$P = \frac{p_\parallel + 2p_\perp}{3}, \tag{A9}$$

where $p_\parallel$ and $p_\perp$ are the parallel and perpendicular thermal pressures defined in magnetic field-aligned coordinate. On the other hand, the anisotropy parameter ξ is defined as

$$\xi \equiv 1 - \frac{p_\parallel - p_\perp}{B^2/\mu_0}. \tag{A10}$$

[92] In the de Hoffmman-Teller frame of reference we can express equations (A1)–(A6) as the downstream to upstream ratios for plasma density (ρ_2/ρ_1), tangential magnetic field (B_{t2}/B_{t1}), and normal and tangential velocity (V_{n1}^*/V_{n2}^* and V_{t2}^*/V_{t1}^*) [*Chao*, 1970]:

$$\frac{\rho_2}{\rho_1} \equiv \frac{1}{y} = \frac{V_{n1}^*}{V_{n2}^*}, \tag{A11}$$

$$\frac{B_{t2}}{B_{t1}} = \left(\frac{m^2 - \cos^2\theta_{BN}}{\sin^2\theta_{BN}}\right)^{1/2} \equiv u, \tag{A12}$$

$$\frac{V_{t2}^*}{V_{t1}^*} = yu \equiv z, \tag{A13}$$

where the normal component of the magnetic field B_n is conserved. From the definition of m and β, the downstream to upstream ratio of the pressure (P_2/P_1) can be expressed as

$$\frac{P_2}{P_1} = m^2\frac{\beta_2}{\beta_1} \equiv v. \tag{A14}$$

Moreover, dividing (A6) by $\rho V_{n1}^* V_{t1}$ and with a help from expressions (A11)–(A13), we can obtain expression (11) for the normal Alfvén Mach number M_{AN}.

[93] The velocities are required to be in the same direction as the magnetic fields in the de Hoffmman-Teller frame; thus we can write the upstream and downstream velocities as

$$\mathbf{V}_1^* = -V_{n1}^*\hat{n} + V_{t1}^*\hat{t}, \tag{A15}$$

$$\mathbf{V}_2^* = -V_{n2}^*\hat{n} + V_{t2}^*\hat{t}. \tag{A16}$$

The velocity difference is thus $\mathbf{V}_2^* - \mathbf{V}_1^*$. If $\mathbf{V}_1$ and $\mathbf{V}_2$ are defined as the velocities in the spacecraft frame of reference, then $\mathbf{V}_2 - \mathbf{V}_1 \equiv \mathbf{W} = \mathbf{V}_2^* - \mathbf{V}_1^*$. From equations (A15)–(A16), equations (A11)–(A13) and the definition of the M_{AN}, the **W** can thus be formulated as equation (8). Note that Method A and Method B use the same equation for **W**.

[94] For the normal momentum conservation equation used for Method B, we start from equation (A7). Dividing equation (A7) by $\rho_1 V_{n1}^2$ and with the help of equations (A11)–(A13), one obtains

$$\frac{P_2}{P_1} = 1 + \frac{2\cos^2\theta_{BN}}{\beta_1}\left[\frac{2}{3}(\xi_2 - \xi_1) + \frac{1}{6}(2\xi_2 + 1)\tan^2\theta_{BN} - \Delta G M_{AN}^2 - (y-1)M_{AN}^2 - \frac{1}{6}(2\xi_2+1)u^2\tan^2\theta_{BN}\right], \tag{A17}$$

where ΔG is defined in equation (18). Substituting equation (A14) into (A17), we obtain equation (9′). On the other hand, equation (10′) can be obtained by combining the normal momentum and energy conservation equations. Dividing equation (A8) by $\rho_1 V_{n1}^3$ and with the help of equations (A11)–(A14), we have a parameter equation. When we substitute (A17) into this equation, equation (10′) is thus obtained.

[95] The equations (9) and (10) used for Method A can be easily obtained by letting the ΔG and ΔQ be zeros in equations (9′) and (10′). It is equivalent to the way that we use equations (A7) and (A8) but without g_n and q_n and follow the derivation in above.

Appendix B: Mach Numbers

[96] The downstream normal Alfvén Mach number is defined as $M_{AN2} = V_{n2}^*/(V_{A2}\cos\theta_{BN2})$, where V_{A2} =

$B_2/(\mu_0\rho_2)^{1/2}$ and $\cos\theta_{BN2} = B_n/B_2$. Substituting these two expressions into M_{AN2} and using the definition of y, we can write the M_{AN2} as equation (19).

[97] From MHD wave theory, it is well known that the upstream fast-mode wave speed is

$$V_F = \frac{1}{\sqrt{2}}\left[\left(V_A^2 + C_S^2\right) + \left[\left(\left(V_A^2 + {C_S}^2\right)^2 - 4C_S^2 V_A^2 \cos^2\theta_{BN}\right]^{1/2}\right]^{1/2}, \tag{B1}$$

where C_S is the sound speed in the plasma. It can be written as $C_S = (\gamma P_1/\rho_1)^{1/2} = (\gamma\beta_1/2)^{1/2} V_A$. While we divide the upstream speed V^*_{1n} by V_F and replace the C_S by $(\gamma\beta_1/2)^{1/2} V_A$, equation (20) for the upstream fast Mach number can be obtained. In the same manner, we obtain the expression in equation (21) for the downstream fast Mach number.

[98] For anisotropic case, it can be shown that the effective upstream normal Alfvén speed equals to $(V_A\xi^{1/2})\cos\theta_{BN}$ [e.g., *Parks*, 1991]. Thus the effective upstream normal Alfvén Mach number is

$$M_{AN}^{(a)} = \frac{M_{AN}}{\xi^{1/2}}. \tag{B2}$$

Likewise, we can derive the effective downstream normal Alfvén Mach number. Moreover, the upstream effective fast-mode speed can be derived under the CGL assumption [*Chew et al.*, 1956].

$$V_F^{(a)} = \frac{1}{\sqrt{2}}\left[a_1 + a_2 + \left[(a_1 - a_2)^2 + 4a^2\right]^{1/2}\right]^{1/2}, \tag{B3}$$

where

$$a_1 \equiv \left(2C_\perp^2 + V_A^2\right)\sin^2\theta_{BN} + \left(V_A^2 + C_\perp^2 - C_\parallel^2\right)\cos^2\theta_{BN}, \tag{B4}$$

$$a_2 \equiv 3C_\parallel^2 \cos^2\theta_{BN}, \tag{B5}$$

$$a \equiv C_\perp^2 \sin\theta_{BN}\cos\theta_{BN}. \tag{B6}$$

Here, $C_\parallel \equiv p_{1\parallel}/\rho_1$ and $C_\perp \equiv p_{1\perp}/\rho_1$. They can be rewritten as follows.

$$C_\parallel = \left[\frac{C_S^2}{\gamma} + \frac{2}{3}(1 - \xi_1)V_A^2\right]^{1/2}, \tag{B7}$$

$$C_\perp = \left[\frac{C_S^2}{\gamma} - \frac{1}{3}(1 - \xi_1)V_A^2\right]^{1/2}. \tag{B8}$$

Dividing V^*_{1n} by $V_F^{(a)}$, we can derive the effective upstream fast Mach number. In the same manner, we can derive the expression for the effective downstream fast Mach number.

Appendix C: Perpendicular Shock

[99] For a perpendicular shock, equations (A11)–(A13) can be reduced to $z = 1$ and $u = m = 1/y$. In the shock frame of reference, there is no jump in tangential component of the velocity. So, the velocity difference, W, can be calculated as

$$\mathbf{W} = \mathbf{V}_2' - \mathbf{V}_1' = -\left(V_{n2}' - V_{n1}'\right)\hat{n}, \tag{C1}$$

where $\mathbf{V}_1'(\mathbf{V}_2')$ is the upstream (downstream) velocity and $V_{n1}'(V_{n2}')$ is the upstream (downstream) normal speed in the shock frame of reference. Note that the $V_{n1}'(V_{n2}')$ equals to $V^*_{n1}(V^*_{n2})$. Thus from equation (A11) and the definition of M_A ($=V^*_{n1}/V_A$), we can obtain

$$\mathbf{W} = M_A V_A (1 - y)\hat{n}. \tag{C2}$$

[100] For a perpendicular shock, $B_n = 0$ and $B = B_t$. Dividing the normal momentum equation (A7) (with $g_n = 0$) by $\rho_1 V_{n1}^2$, we can obtain

$$\beta_1 = \frac{2}{1 - v}\left((y - 1)M_A^2 + \frac{1}{2y^2} - \frac{1}{2}\right), \tag{C3}$$

where $v \equiv P_2/P_1$, which is expressed in equation (A14). Using equation (A14), the above expression can be rewritten as

$$\beta_2 = y^2\left[\beta_1 - 2\left((y - 1)M_A^2 + \frac{1}{2y^2} - \frac{1}{2}\right)\right]. \tag{C4}$$

On the other hand, equation (A8) (with $q_n = 0$) is divided by $\rho_1 V_{n1}^3$ to obtain

$$\frac{5}{2}\beta_1(1 - vy) = \left(y^2 - 1\right)M_A^2 + \frac{2}{y}(1 - y). \tag{C5}$$

Combining equations (C3) and (C5), we can have

$$\beta_1 = \frac{2}{5}(4y - 1)M_A^2 - \frac{1}{5y}(1 + 5y). \tag{C6}$$

Equations (C4) and (C6) can be used to determine β_1 and β_2 for a perpendicular shock, if the values of M_A and y are given.

[101] For the fast Mach numbers, dividing the V_{n1}' and V_{n2}' by equation (B1) (with $\cos\theta_{BN} = 0$), respectively, and replacing the C_S by $(\gamma\beta_1/2)^{1/2} V_A$, we obtain

$$M_F = \frac{M_A}{\sqrt{(1 + \gamma\beta_1/2)}}, \tag{C7}$$

$$M_{F2} = \frac{M_A\sqrt{y}/m}{\sqrt{(1 + \gamma\beta_2/2)}}. \tag{C8}$$

[102] For the synthetic perpendicular shock in section 3.3, we set $y = 2/3$ ($N_{eq1} = 8$ and $N_{eq2} = 12$) and $M_A = 2$. Moreover, for simplicity we choose B_1 and B_2 to lie on the Y-GSE direction. Since $m = 1/y = 3/2$, if we choose $B_{1y} = -10$ nT, then $B_{2y} = -15$ nT. The other components are zero. Also for simplicity, we choose the shock normal to lie on the x-GSE direction and point toward Earth. Thus with the values given, we can obtain the values of V_A, **W**, β_1, β_2, M_F,

and M_{F2} from equations (7), (C2), (C6), (C4), (C7), and (C8). The associated values are listed in Table 7.

[103] For this case, we arbitrarily let the upstream plasma velocity seen by spacecraft be $\mathbf{V}_1 = (-430, 10, 10)$ km/s. Then the downstream flow velocity can be obtained from $\mathbf{V}_2 = \mathbf{V}_1 + \mathbf{W} = (-481.4, 10, 10)$ km/s. For the shock propagation speed, we also assume that two spacecraft have a displacement vector of $\Delta\mathbf{R} = (-100, 100, 0)\, R_E$. Therefore with equation (15), we have the shock speed in the spacecraft frame of reference versus= 584.2 km/s. We also have the difference between shock arrival times, Δt = 18.2 min. The values are also listed in Table 7.

Appendix D: Slippage Pressure Tensor in Solar Wind

[104] The slippage pressure tensor is contributed by interspecies velocity difference. In the solar wind, velocity differences between the solar wind protons and alpha particles have been measured by ISEE 3 spacecraft along its orbit [*Ogilvie et al.*, 1982]. Sometimes, cases of slippage of alpha particles relative to proton fluid at a speed on the order of one Alfvén wave speed were found, but it is not a common situation. From an investigation covering a full range of solar wind conditions, *Ogilvie et al.* [1982] suggested that for solar wind velocities between 300 and 400 km/s the alpha particles have a larger velocity than protons by 5 km/s on average, and for solar wind velocities between 400 and 500 km/s the difference is ~14 km/s.

[105] From kinetic theory one can obtain a kinetic tensor, which contains of the ram pressure and thermal pressure, by integrating the distribution functions of each species. It can be expressed as

$$\sum_{\alpha} \iiint m_\alpha f_\alpha v_i v_j d^3v = \sum_{\alpha} \rho_\alpha V_{\alpha i} V_{\alpha j} + \sum_{\alpha} p_{\alpha,ij}, \qquad \text{(D1)}$$

where α represents the particle species in solar wind, and i and j represent the components in any coordinate system. Here, the $p_{\alpha,ij}$ on the right hand side of equation (D1) is the thermal pressure tensor for each species in their own center of mass system. It is obtained by integrating the distribution function in the frame of each species. The thermal pressure tensor P_{ij} in our system equals to $\sum_{\alpha} p_{\alpha,ij}$, where α represents proton, electron and alpha particle. If we integrate the same distribution function in the frame of the center of mass of all species, the integration in (D1) can be expressed as

$$\sum_{\alpha} \iiint m_\alpha f_\alpha v_i v_j d^3v = \rho V_i V_j + P_{ij}^{CM}. \qquad \text{(D2)}$$

Here, $\rho = \sum_{\alpha} \rho_\alpha$, and V_i (V_j) is the center of mass velocity. P_{ij}^{CM} represents the "total" pressure tensor obtained by integrating the distribution function in the center of mass of the plasmas. Equations (D1) and (D2) are equivalent. That is, the "total" pressure tensor can be expressed as

$$P_{ij}^{CM} = \sum_{\alpha} p_{\alpha,ij} + \left(\sum_{\alpha} \rho_\alpha V_{\alpha i} V_{\alpha j} - \rho V_i V_j \right). \qquad \text{(D3)}$$

Then, the terms in the parentheses represent the difference between the "total" pressure tensor and the thermal pressure tensor. We now define this difference as a slippage pressure tensor, π_{ij}. It is written as follows.

$$\pi_{ij} ij^{CM} - \sum_{\alpha} p_{\alpha,ij} = \sum_{\alpha} \rho_\alpha V_{\alpha i} V_{\alpha j} - \rho V_i V_j \qquad \text{(D4)}$$

In addition, the slippage pressure tensor can also be expressed as

$$\pi_{ij} = \sum_{\alpha} \rho_\alpha (V_{\alpha i} - V_i)(V_{\alpha j} - V_j). \qquad \text{(D5)}$$

Knowing the density and bulk velocity of each species, we can evaluate this tensor.

[106] For slippage pressure tensor in solar wind, we consider only the slippage of alpha particles from protons. For convenience, we further write (D5) as

$$\pi_{ij} = \frac{\rho_p \rho_a}{\rho_p + \rho_a} \left[(V_{pi} - V_{ai})(V_{pj} - V_{aj}) \right]. \qquad \text{(D6)}$$

[107] **Acknowledgments.** This work was supported by the National Science Council of China under grants NSC 93-2111-M-008-003, 94-2111-M-008-034, and NSC 95-2111-M-008-037 to the National Central University and under grant NSC 94-2111-M-006-002 to the National Cheng Kung University. The authors thank NASA/GSFC for the use of the key parameters from WIND and Geotail obtained via the CDA Web page and would also like to thank the M.I.T. Space Plasma Group for the use of their high-resolution WIND magnetic field data obtained via the WIND-SWE Data Page. The authors also thank Jack D. Scudder for providing his constructive comments and suggestions.

[108] Shadia Rifai Habbal thanks Daniel Berdichevsky, Barbara Abraham-Shrauner, and another reviewer for their assistance in evaluating this paper.

References

Abraham-Shrauner, B. (1972), Determination of magnetohydrodynamic shock normals, *J. Geophys. Res.*, *77*, 736.

Abraham-Shrauner, B., and S. H. Yun (1976), Interplanetary shocks seen by AMES plasma probe on pioneer 6 and 7, *J. Geophys. Res.*, *81*, 2097.

Berdichevsky, D. B., A. Szabro, R. P. Lepping, and A. F. Viñas (2000), Interplanetary fast shocks and associated drivers observed through the 23rd solar minimum by Wind over its first 2.5 years, *J. Geophys. Res.*, *105*, 27,289.

Chao, J. K. (1970), Interplanetary collisionless shock waves, *Rep. CSR TR-70–3*, Mass. Inst. of Technol., Cent. for Space Res., Cambridge.

Chao, J. K., and B. Goldstein (1972), Modification of the Rankine-Hugoniot relations for shocks in space, *J. Geophys. Res.*, *77*, 5455.

Chao, J. K., and K. C. Hsieh (1984), On determining magnetohydrodynamic shock parameters θ_{Bn} and M_A, *Planet. Space Sci.*, *32*, 641.

Chao, J. K., X. X. Zhang, and P. Song (1995), Derivation of temperature anisotropy from shock jump relations: Theory and observations, *Geophys. Res. Lett.*, *22*, 2409.

Chew, G. F., M. L. Goldberger, and F. E. Low (1956), The Boltzmann equation and the one-fluid hydromagnetic equations in the absence of particle collisions, *Proc. R. Soc. London, Ser. A*, *236*, 112.

Coates, A. J., A. D. Johnstone, R. L. Kessel, and D. E. Huddleston (1990), Plasma parameters near the comet Halley bow shock, *J. Geophys. Res.*, *95*, 20,701.

Colburn, D. S., and C. P. Sonett (1966), Discontinuities in the solar wind, *Space Sci. Rev.*, *5*, 439.

Davison, R. C., and N. A. Krall (1977), Anomalous transport in high-temperature plasmas with applications to solenoidal fusion system, *Nucl. Fusion*, *17*, 1313.

Dryer, M., Z. K. Smith, G. H. Enrudd, and J. H. Wolfe (1972), Pioneer 7 observations of the August 29, 1966, interplanetary shock ensemble, *Cosmic Electrodyn.*, *3*, 184.

Giacalone, J., D. Burgess, S. J. Schwartz, D. C. Ellison, and L. Bennett (1997), Injection and acceleration of thermal protons at quasi-parallel

shocks: A hybrid simulation parameters survey, *J. Geophys. Res.*, *102*, 19,789.
Kessel, R. L., A. J. Coates, U. Motschmann, and F. M. Neubauer (1994), Shock normal determination for multiple-ion shocks, *J. Geophys. Res.*, *99*, 19,359.
Knetter, T., F. M. Neubauer, T. Horbury, and A. Balogh (2003), Discontinuity observations with cluster, *Adv. Space Res.*, *32*(4), 543.
Knetter, T., F. M. Neubauer, T. Horbury, and A. Balogh (2004), Four-point discontinuity observations using Cluster magnetic field data: A statistical survey, *J. Geophys. Res.*, *109*, A06102, doi:10.1029/2003JA010099.
Lepping, R. P. (1972), Influence of thermal anisotropy on best fit estimates of shock normals, *J. Geophys. Res.*, *77*, 2957.
Lepping, R. P., and P. D. Argentiero (1971), Single spacecraft method of estimating shock normals, *J. Geophys. Res.*, *76*, 4349.
Lepping, R. P., and K. W. Behannon (1980), Magnetic field directional discontinuities: 1. Minimum variance errors, *J. Geophys. Res.*, *85*, 4695.
Lepping, R. P., et al. (1997), The Wind magnetic cloud and events of October 18–20, 1995: Interplanetary properties and as trigger for geomagnetic activity, *J. Geophys. Res.*, *102*, 14,049.
Lyu, L. H., and J. R. Kan (1986), Shock jump conditions modified by pressure anisotropy and heat flux for Earth's bowshock, *J. Geophys. Res.*, *91*, 6771.
Ogilvie, K. W., and L. F. Burlaga (1969), Hydromagnetic shocks in the solar wind, *Sol. Phys.*, *8*, 422.
Ogilvie, K. W., M. A. Coplan, and R. D. Zwickl (1982), Helium, hydrogen, and oxygen velocities observed on ISEE 3, *J. Geophys. Res.*, *87*, 7363.
Parks, G. K. (1991), *Physics of Space Plasmas: An Introduction*, Addison-Wesley, Boston, Mass.
Press, W. H., S. A. Teukolsky, W. T. Vetterling, and B. P. Flannery (1992), *Numerical Recipes in Fortran*, 2nd ed., Cambridge Univ. Press, New York.
Russell, C. T., M. M. Mellott, E. J. Smith, and J. H. King (1983), Multiple spacecraft observations of interplanetary shocks: Four spacecraft determination of shock normals, *J. Geophys. Res.*, *88*, 4739.
Scudder, J. D. (2005), Geometry of magnetosonic shocks and plane-polarized waves: Coplanarity variance analysis (CVA), *J. Geophys. Res.*, *110*, A02202, doi:10.1029/2004JA010660.
Sonnerup, B. U. Ö, and L. T. Cahill Jr. (1967), Magnetopause structure and attitude from Explorer 12 observations, *J. Geophys. Res.*, *72*, 171.
Sonnerup, B. U. Ö., et al. (2004), Orientation and motion of a discontinuity from single-spacecraft measurements of plasma velocity and density: Minimum mass flux residue, *J. Geophys. Res.*, *109*, A03221, doi:10.1029/2003JA010230.
Szabo, A. (1994), An improved solution to the "Rankine-Hugoniot" problem, *J. Geophys. Res.*, *99*, 14,737.
Szabo, A., and R. P. Lepping (1995), Neptune inbound bow shock, *J. Geophys. Res.*, *100*, 1723.
Tsai, C. L., R. H. Tsai, B. H. Wu, and L. C. Lee (2002), Structure of slow shocks in a magnetized plasma with heat conduction, *Phys. Plasmas*, *9*, 1185.
Tsai, C. L., B. H. Wu, and L. C. Lee (2005), Structure of intermediate shocks and slow shocks in a magnetized plasma with heat conduction, *Phys. Plasmas*, *12*, 082501.
Viñas, A. F., and J. D. Scudder (1986), Fast and optimal solution to the "Rankind-Hugoniot problem", *J. Geophys. Res.*, *91*, 39.
Winterhalter, D., M. G. Kivelson, R. J. Walker, and C. T. Russell (1985), Magnetic field change across the Earth's bow shock: Comparison between observations and theory, *J. Geophys. Res.*, *90*, 3925.
Wu, D. J., J. K. Chao, and R. P. Lepping (2000), Interaction between an interplanetary magnetic cloud and the Earth's magnetosphere: Motions of the bow shock, *J. Geophys. Res.*, *105*, 12,627.
Yoon, P. H., and T. Y. Lui (2006), Quasi-linear theory of anomalous resistivity, *J. Geophys. Res.*, *111*, A02203, doi:10.1029/2005JA011482.

J. K. Chao, L. C. Lee, C. C. Lin, and L. H. Lyu, Institute of Space Science, National Central University, Taiwan 32001, R.O.C. (dannylin@jupiter.ss.ncu.edu.tw)
D. J. Wu, Purple Mountain Observatory, Academic Sinica, Nanjing 210008, China.